Impact Modeling and Estimation for Multi-Arm Space Robot while Capturing Tumbling Orbiting Objects

A Thesis submitted by

Deepak Raina

in partial fulfillment of the requirements for the award of the degree of

Master of Technology

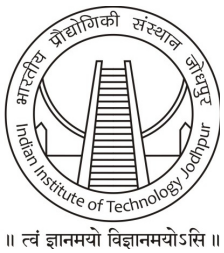

Indian Institute of Technology Jodhpur

Department of Mechanical Engineering

June 2017

Declaration

I hereby declare that the work presented in this thesis titled *Impact Modeling and Estimation for Multi − Arm Space Robot while Capturing Tumbling Orbiting Objects* submitted to the Indian Institute of Technology Jodhpur in partial fulfilment of the requirements for the award of the degree of *Master of Technology*, is a bonafide record of the research work carried out under the supervision of *Dr. Suril Vijaykumar Shah*. The contents of this thesis in full or in parts, have not been submitted to, and will not be submitted by me to, any other Institute or University in India or abroad for the award of any degree or diploma.

Deepak Raina

M15ME003

Certificate

This is to certify that the thesis titled *Impact Modeling and Estimation for Multi − Arm Space Robot while Capturing Tumbling Orbiting Objects*, submitted by *Deepak Raina* (*M15ME003*) to the Indian Institute of Technology Jodhpur for the award of the degree of Master of Technology, is a bonafide record of the research work done by him under my supervision. To the best of my knowledge, the contents of this report, in full or in parts, have not been submitted to any other Institute or University for the award of any degree or diploma.

Suril Vijaykumar Shah

M.Tech. Thesis Supervisor

Abstract

Autonomous on-orbit services, such as capturing, refueling, and repair and refurbishment of an on-orbit satellite using a robot mounted on service satellite, will be one of the important components of the space missions in future. The main objective of capturing faulty satellites/debris is to avoid their possible collision with a working satellite in the same orbit. Use of space robots boosts the reliability, safety, and ease of execution of operations. Driven by this motivation, an attempt has been made in this work to develop a framework for impact modeling of a multi-arm robotic system mounted on a servicing satellite while the capture of tumbling orbiting objects. A robotic system with multiple arms would be capable of capturing multiple objects simultaneously. Further, when the satellite is in broken state or does not have provision for grapple and tumbling, the interception is very difficult. In such cases, interception using multi-arm robotic system can be appealing as this will increase the probability of grasp in comparison to the single-arm robot. In this work, three phases of the capturing operation, namely, approach, impact, and post-impact have been modeled. In the approach phase, the robot is traveled from its initial configuration to the desired configuration. It is essential that at the time of interception the velocity of the end-effector should be equal to that of the point to be grasped in order to avoid any impact. Hence, the main objective in approach phase is to move end-effector from point-to-point with desired final velocity. But in practice, there will be a non-zero relative velocity between the end-effector and the grapple point, leading to an impact. In the impact phase, a framework is developed to estimate the changes in the generalized velocities caused by the impact. In post-impact phase, these velocities are used as an initial condition for the post impact dynamics simulations. Efficacy of the framework is shown using a dual-arm robot mounted on a servicing satellite performing capturing operation for two objects, in the case of open-loop impact and for the single object, in the case of closed-loop impact. The effects of relative velocity and angle of approach on the impact forces have been investigated.

Acknowledgments

When I look back at my M.Tech years it amazed me and at the same time I am thankful for all I have received throughout these years. This period has shaped me as a person and has steered me to where I am now.

I would like to express my deep and sincere gratitude to my supervisor, *Professor Suril Vijaykumar Shah*, for his invaluable guidance and support. He has always encouraged me to work intensively, even when I was thinking about doing something else. He has enlightened me through his wide knowledge of multibody dynamics and his deep intuitions about where it should go. His knowledge and logical way of thinking has been of great value for me. Without his encouragement and constant guidance, realization of this thesis would have not been possible.

Far too many people to mention individually have assisted in so many ways during my work at IIT Jodhpur. They all have my sincere gratitude. In particular, I would like to thank *Mr. Mithun* and *Mr. A. Venu Gopal*, all currently or previously stayed for their research work or project in the Robotics Laboratory of IIT Jodhpur. I would also like to thank friends *Mr. Pratik* and Mr. *Shravan* for the time we spent together after the laboratory hours. My thanks are also due to all the office staff of the department for their kind support and co-operation.

I am thankful to all my family members and friends for helping me in innumerable ways. Specially, I thank my sister *Jyoti* for her constant encouragement throughout this period. Penultimate thanks go to my wonderful parents, for always being there when I needed them most, and never complaining about how infrequently I visited them. They deserve far more credit than I can ever give them.

Contents

		page
Abstract		*i*
Acknowledgements		*iii*
Contents		*v*
List of Figures		*vii*
List of Tables		*ix*
List of Symbols		*xi*
List of Abbreviations		*xiii*
Chapter 1:	**Introduction**	1
1.1	Motivation	1
1.2	Background and literature survey	2
1.2.1	*Robotic Systems*	*2*
1.2.2	*Dynamic Modeling*	*3*
1.2.3	*Equations of Motion*	*4*
1.2.4	*Impact Modeling*	*6*
1.2.5	*Thesis Objectives*	*8*
1.2.6	*Summary*	*8*
1.3	Thesis Organization	9
Chapter 2:	**Kinematic and Dynamic Modeling of Multi-Arm Robot and Target**	11
2.1	Kinematics of Multi-Arm Robot	11
2.2	Dynamics of Open Multi-Arm Robot	14
2.3	Dynamics of Closed Multi-Arm Robot	15
2.4	Target Dynamics	16
2.5	An Illustration	18
Chapter 3:	**Impact Model**	19
3.1	Pre-Impact Phase	20
3.2	Impact Phase	20

3.2.1 Impact Force Estimation 21
3.3 Post-Impact Phase 22
3.3.1 Velocity Estimation 22

Chapter 4: Results and Discussion 25
4.1 Open Loop Impact 26
4.2 Closed Loop Imapct 33
4.3 Impact Investigation 36

Chapter 5: Conclusion and Future work 41
5.1 Future Work 42

Chapter A: Kinematic Equations of Dual-arm space robot 43
A.1 Position kinematics 43
A.2 Velocity Kinematics 44

Appendix B: Dynamical Equations of Dual-arm space robot 47
B.1 Equations of Motion using DeNOC 47
B.2 Matrix Formulation 51

Appendix C: Momentum Conservation Equations 55
C.1 Linear Momentum 56
C.2 Angular Momentum 57
C.3 Matrix Formulation 58

References 59

List of Figures

Figures	*Title*	*page*
1.1	A PUMA industrial robot (fixed base)	3
1.2	A Space Robot (floating base) (Dimitrov, 2006)	3
2.1	A multi-arm robotic system mounted on a service satellite. The robot has r arms and the j_{th} arm has n_j links and n_j joints. Mass and inertia tensor of the k_{th} link on the j_{th} arm are denoted by $m_{j,k}$ and $I_{j,k}$, respectively. p and l are the linear and angular momenta, respectively. The total degree of freedom of the system is $n_1 + ... + n_r = n$	12
2.2	A free-floating target object	17
2.3	Schematic diagram of multi-arm space robot	18
4.1	Schematic diagram of multi-arm robot and target	25
4.2	Pre-impact initial configuration	28
4.3	Impact phase configuration	28
4.4	Actual joint angles	29
4.5	End-effector velocity	29
4.6	Impact phase velocities	30
4.7	Total momentum before impact	30
4.8	Both target rotating CCW	31
4.9	Both target stationary	31
4.10	Target 1 rotating CCW and target 2 CW	32
4.11	One target stationary	32

4.12 Total momentum after impact 33

4.13 Pre-impact initial configuration 35

4.14 Impact phase configuration 35

4.15 Post impact dynamics 36

4.16 Loop closure violation 36

4.17 Different angles of approach in open-loop systems 37

4.18 Impulse in open-loop systems 38

4.19 Different angles of approach in closed-loop systems 39

4.20 Impulse in closed-loop systems 39

C.1 A robotic system mounted on a floating or mobile base (Dimitrov, 2006) 55

List of Tables

Figures	*Title*	*page*
4.1	Model parameters of dual-arm robot and base	26
4.2	Model parameters of target	26
4.3	Desired initial and final joint angles	27
4.4	Initial and final end-effectors' position	27
4.5	Desired initial and final joint angles	34
4.6	Initial and final end-effectors' position	34
4.7	Impulse (N-s) estimation	37

List of Symbols

Symbol	*Description*
C	Matrix of Convective Inertia (MCI) terms
F_e	6-dimensional vectors of moments and forces exerted on the centroid of end-effectors
I_b	6×6 inertia matrix of the floating-base
I_t	6×6 inertia matrix of target object
I_t^c	3×3 centroidal inertia tensor of target object
I_{bm}	$6 \times n$ coupling inertia matrices
I_m	$n \times n$ inertia matrices of manipulator
J_t	6×6 Jacobian matrix of target object
J_b	6×6 Jacobian matrix from base to the end-effector of the manipulator
J_m	$6 \times n$ Jacobian matrix for the manipulator
M	Generalized mass matrix
$N_l^T N_d^T$	Link-level Decoupled Natural Orthogonal Complement (DeNOC) matrices
R_{tb}	Cross-product tensor associated with r_{tb}
Ω	Angular velocity matrix
$\ddot{\theta}$	n-dimensional joint acceleration vector
$\dot{t}_t$	6-dimensional linear and angular acceleration vector of target object
$\dot{t}_b$	6-dimensional vector of linear and angular acceleration of the base
λ	Vector of Lagrange multipliers
ω_t	3-dimensional angular velocity vector of target object

Symbol	Description
$\overline{F}$	6-dimensional vector of linear and angular impulse
τ_m	6-dimensional vector of manipulator joint torques
τ_t	6-dimensional vector of generalized moments and forces exerted on target object
θ_e	End-effector orientation i.e. angle of approach
c_0	3-dimensional position vector of center-of-mass
c_b	6×1 velocity dependent nonlinear term associated with the base
c_m	6×1 velocity dependent nonlinear term associated with the manipulator
f_b	6-dimensional vectors of moments and forces exerted on the centroid of base
l	3-dimensional angular momentum vector
p	3-dimensional linear momentum vector
r_{tb}	3-dimensional position vector from COM of the target to the point of contact
t	6-dimensional vectors of twist
t_b	6-dimensional twist vector constituting linear and angular velocities of the base
v_t	3-dimensional linear velocity vector of target object
w	$6n-$ dimensional generalized wrenches
w^C	Vector of generalized constraint wrenches
w^D	Vector of generalized driving wrenches
w^E	Vector of generalized external wrenches
$\dot{\theta}_i$	n-dimensional joint velocities vector of the i-th manipulator
m_t	Mass of target object

List of Abbreviations

Symbol	*Description*
COM	Centre-of-Mass
DAE	Differential Algebraic Equations
DeNOC	Decoupled Natural Orthogonal Complement
DOF	Degrees-of-freedom
EL	Euler-Lagrange
EOM	Equations-of-Motion
GIM	Generalized Inertia Matrix
GJM	Generalized Jacobian Matrix
MOI	Moment of Inertia
NE	Newton-Euler
OOS	On-Orbit Servicing
PD	Proportional and Derivative
ReDySim	Recursive Dynamics Simulator

1
Introduction

1.1 MOTIVATION

Space robotics have been an active area of research for the last few years (Sellmaier et al., 2010; Liou, 2011). Particularly, On-Orbit Servicing (OOS) is one of the areas in space robotics that is gaining researchers' attention due to its commercial drive. These OOS will be carried out autonomously using a satellite mounted robotic systems. OOS involves rendezvous, proximity operations, and capture, berthing or docking. Use of robots boosts the reliability, safety, and ease of execution of operations after proximity operations. The present work mainly focuses on orbital detritus management, which involves the autonomous capture of orbiting objects such as space debris. This space debris can cause significant damage if it collides with a working satellite in the same orbit. Hence, orbital detritus management is gaining importance in the recent years. The Autonomous capture of orbiting object is a challenging task, as one must ensure that there is no or minimum impact at the end of capture phase. Any undesired impact will generate large forces and moments, and destabilize the attitude of the base satellite (Yoshida and Sashida, 1993; Wee and Walker, 1993; Cyril et al., 2000). This may cause damage to the internal component of the satellite and require additional fuel for its attitude control. Therefore, the ultimate goal is to keep impact minimum while capture by ensuring zero relative velocity between end-effector and grapple point at the time of capture (Yoshida et al., 2006). This, however, is a difficult task when the object is tumbling as the end-effector cannot achieve velocity beyond a certain limit without change in the attitude of the base satellite. Practically, there always exists a velocity difference and resulting impact. Alternatively, one may ensure that impact force passes through

the center-of-mass of the system as this will minimize attitude disturbance of the satellite. This will require correct estimation of impact forces. Estimation of impact forces will also help in post-impact control. Therefore, impact modeling and estimation is very important. This work focuses on impact modeling while the capture of debris. The entire capture operation includes three phases, namely approach, impact and post impact. The successful capture of an orbiting tumbling object using a space manipulator depends on how perfectly these three phases have been modeled.

In this thesis, a framework has been developed for impact modeling and estimation for the multi-arm space robot.

1.2 BACKGROUND AND LITERATURE SURVEY

The field of robotics has grown a lot in last 3-4 decades. In this chapter, background and brief overview of the literature survey conducted during this research is presented.

1.2.1 Robotic Systems

A robotic system can be divided into two categories based on their topology, i.e., fixed base and floating base system. A robot is said to have a fixed base if it is rigidly attached to a fixed support, e.g., a PUMA industrial robot arm is a good example of a fixed-base robot as shown in Fig. 1.1. If no part of the robot mechanism is fixed, then it is said to have a floating base. Wheeled and legged mobile robots, flying robots, swimming robots, space robots and humanoids are all floating-base robots. The space robot working on a satellite is shown in Fig. 1.2. In a floating-base robot, one particular link is identified as the floating base. Usually, it is the largest or heaviest link. A floating base robot can further act as open-loop and closed-loop systems. Robots with serial and tree-type architecture are open-chain systems, whereas the analysis of closed-chain systems can be carried out by cutting appropriate joints to form a tree-type system, where the opened joints are substituted by constraint forces. This thesis addresses the dynamics and impact modeling of an open- and closed-loop floating-base robotic systems.

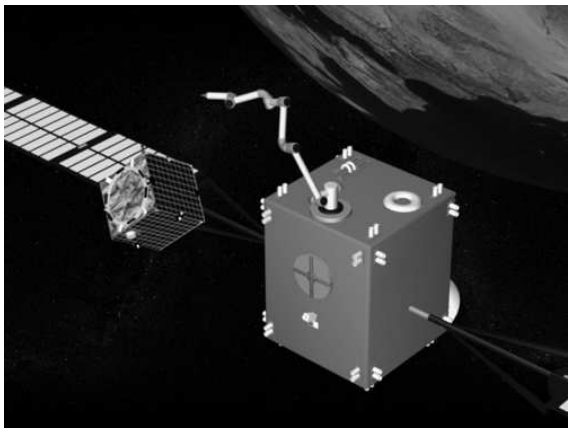

Figure 1.1. : A PUMA industrial robot (fixed base) **Figure 1.2. :** A Space Robot (floating base) (Dimitrov, 2006)

1.2.2 Dynamic Modeling

Since the evolution of high-speed computing facilities, computer-aided dynamic analysis of robotic systems has been a prime motive of the engineers. In order to perform computer-aided analysis, the actual system is represented by its dynamic model, which has information in terms of link parameters, joint variables and constraints. A Dynamic model of a robotic system is represented by a set of equations governed by physical laws of motions. For a system with few links, it is easier to obtain explicit expressions for the equations of motion. However, finding equations of motion is not an easy task for complex systems with many links. Sometimes even with 4 or 5 links, say, a 4-bar mechanism, it is difficult to find an explicit expression for the system inertia in terms of the link length, mass and joint angle. Various techniques are available in the literature for automatic generation of the equations of motion. Development of the equations of motion is an essential step for dynamic analysis. There are two types of dynamic analysis. First is inverse dynamics, i.e. to perform force analysis, in which driving forces of the system are computed for a given set of input joint motions. Knowledge of the driving forces helps not only in control, but also in actuator design of the robot. One may also obtain the reaction forces, which may be used for design of associated linkages and joints from the strength point of view. Second is forward dynamics, i.e.

motion analysis, where joint motions are computed under the application of driving forces. This along with numerical integration helps in obtaining the configuration or state of the system at any instant of time. In other word forward dynamics problem lets one to simulate the actual working of the system.

With the evolution of complex robotic systems and continuous development in the field of robotics, application of multibody dynamics has still wider scope of research in the field of robotics. Over the last two decades, applications of multibody dynamics have grown in the fields of robotics, automobile, aerospace, bio-mechanics, molecular modeling and many more. History of dynamics goes back to the seventeenth century when Newton in 1686 presented the dynamics of a free particle and later Euler in 1776 introduced the concept of rigid bodies. This gave birth to Newton-Euler equations of motion. Lagrange in 1788 provided the systematic approach for the mathematical formulation of the constrained rigid body systems. Since then multibody dynamics have grown a lot. A Comprehensive discussion on dynamic formalisms can be found in the seminal text by Schwertassek and Roberson (1988), Schiehlen et al. (1990), Stejskal and Valášek (1996), and Wittenburg (2007). Recent trends in dynamic formalisms can also be found in the work by Schiehlen (1997), Featherstone and Orin (2000) and Eberhard and Schiehlen (2006).

1.2.3 Equations of Motion

Dynamic modeling is referred as the derivation of the equations of motion in order to study the dynamics of any system. There are several fundamental methods of formulating equations of motion. For example, Newton-Euler (NE), Euler-Lagrange (EL) principle, Gibbs-Appel approach, Kane's method, and D'Alembert's principle. All the above mentioned approaches, when applied to robotic systems, have their own advantages and disadvantages. NE approach is one of the classical methods for dynamic formulation. This approach is based on the concept of "free-body". If it is constrained, associated forces of constraints are included in the free-body with those, which are externally applied. Mathematically, NE equations of motion lead to two vector equations, which in

scalar form is equivalent to three translational equations of motion of the Centre-of-Mass (COM), and three equations determining the rotational motion of the rigid body. The NE equations are related simply by the constraint forces and hence for an open-chain system they can easily be solved recursively. EL formulation is another classical approach widely used for dynamic modeling. The EL formulation uses the concept of generalized co-ordinates instead of Cartesian co-ordinates. It is based on minimization of a function called "Lagrangian" which is nothing but the difference between kinetic energy and potential energy of the system at hand. Kane's formulation, which is same as the Lagrange's form of D'Alembert's principle, has also been used by few researchers for the development of the equations of motion. It is found to be more beneficial than other formulations when used for systems with nonholonomic constraints.

Typically, EL and NE equations of motion are used for dynamic modeling of a mechanical system. With the advent of digital computers, various other recursive and non-recursive formulations (Eberhard and Schiehlen, 2006; Hollerbach, 1980; Orin and Walker, 1982) have emerged. Recursive formulations are attractive due to their simplicity and computational uniformity regardless of how complex the system is. In the field of robotics, recursive formulations have helped in achieving real-time computations. Saha (1997) proposed one such recursive formulation for the serial-chain systems, which is based on the Decoupled Natural Orthogonal Complement (DeNOC) matrices and theories of linear algebra. The DeNOC matrices are nothing but the decoupled form of a velocity transformation matrix. In this work, dynamics is proposed using the concept of DeNOC matrices, which, when, combined with the uncoupled NE equations of motion give rise to the minimal-order constrained dynamic equations of motion of the system at hand by eliminating the constraint forces. This decoupled form in the DeNOC matrices brings the benefits, as given in Shah et al. (2012a), like analytical expressions of the elements of the vectors and matrices that appear in the dynamic equations of motion, decomposition of the inertia matrix giving deeper insight into the associated dynamics, unified development of recursive inverse and forward dynamics algorithms, etc. To perform dynamic simulation in this work, we have used ReDySim, a MATLAB-based solver (Shah

et al., 2012b), which is a general purpose platform, essentially consisting of very efficient recursive order (n) inverse and forward dynamics algorithms for simulation and control of a tree-type system. ReDySim delves upon the DeNOC approach. The specialty of this solver exists in its recursive nature and flexibility in solving complex problems. Even though, the algorithms in ReDySim are meant for the floating-base open-loop systems, its capability is enhanced to simulate floating-base closed-loop systems.

1.2.4 Impact Modeling

Impact is a complex phenomenon that occurs when two or more bodies undergo a collision (Riley and Sturges, 1996). This phenomenon is important in many different areas such as machine design, robotics, multi-body dynamics. Characteristics of impact are very brief duration, high force levels reached, rapid dissipation of energy and large accelerations and deceleration present. These facts must be considered during the design and analysis of any mechanical system. The Impact of two bodies is characterized by large reaction forces and changes in velocities of the two bodies. As a consequence, the bodies are subject to elastic and/or plastic deformation, with the dissipation of energy in various forms (Goldsmith, 1960). There are two general types of collisions in physics: elastic and inelastic. An inelastic collision occurs when two objects collide and do not bounce away from each other. Momentum is conserved, because the total momentum of both objects before and after the collision is the same. However, the kinetic energy is not conserved. Some of the kinetic energy is converted into sound, heat, and deformation of the objects. A high speed car collision is an inelastic collision. An elastic collision occurs when the two objects bounce apart when they collide. In an elastic collision, both momentum and kinetic energy are conserved. Almost no energy is lost to sound, heat, or deformation. Two rubber balls are a good example.The first rubber ball deforms, but then quickly bounces back to its former shape, and transfers almost all the kinetic energy to the second ball.

The objective of impact modeling is to determine the post-impact conditions of the system,

given its initial (pre-impact) configuration. The impact modeling has been studied widely with respect to fixed-base robots (Zheng and Hemami, 1985; Chapnik et al., 1991), and various models for estimating impulse force during the collision of rigid and flexible robotic arm with environment were developed. The large impulse forces could lead to possible damage of the system. The various strategies for minimizing the impact forces were proposed in Youcef-Toumi and Gutz (1989); Gertz et al. (1991); Walker (1994); Lin et al. (1995). In case of a multi-arm space robot, modeling and estimation of impact may not be straightforward due to the presence of the free-floating base and dynamic coupling between base and arms. Several researchers have studied impact modeling and estimation in space robots (Yoshida and Sashida, 1993; Cyril et al., 1993, 2000; Nenchev and Yoshida, 1999). The impact dynamics for the free-floating multibody system was proposed in Yoshida and Sashida (1993). The work emphasized on modeling the impact dynamics of manipulator subjected to the force impulse at the hand and developed the notion of the Extended-Inverse Inertia Tensor. The inertial effects during the instantaneous impact duration were also taken into account by introducing the virtual rotor inertia model. Further, the impulse index and impulse ellipsoid were presented to express the magnitude and direction of force impulse, which may help in design of the approach phase for minimum impact. In Cyril et al. (1993), the effect of impact due to spinning target on the dynamics of a 2-link space robot was studied, however, it was assumed that at the time of capture there is zero relative velocity between the target and the end-effector, i.e., there is no impact. Later, they studied impact considering non-zero relative velocity and also proposed the post impact control strategy using feedback linearization (Cyril et al., 2000). The impact analysis of a free-floating serial rigid body space robot was studied in Nenchev and Yoshida (1999). The work estimated the reactions occurring at the joints and base in terms of finite velocity changes, which were then used for the post-impact motion control of the space robot.

It is worth noting that the impact modeling of multi-arm space robot is seldom reported to the best of author's knowledge. When a satellite is in broken state or does not have provision for grapple and tumbling, the capturing operation would become very difficult. In such cases,

multi-arm robotic system would be very appealing as it may increase the probability of grasp in comparison to the single-arm robot. In Takahashi et al. (2008), hybrid simulation of dual-arm was presented where the impact forces and moments were estimated from the earth based experimental setup. Impact dynamics of flexible dual-arm robot and feedback control were presented in Liu et al. (2007). The Multi-arm robot can also be used to capture two or more target objects simultaneously, which would enhance the capability of the space robots.

1.2.5 Thesis Objectives

Based on the literature survey, the objectives of the present research are listed below:

1. Comprehensive kinematic and dynamic modeling of pre-impact, impact and post-impact phases for a multi-arm floating base robotics system while capturing tumbling orbiting objects.

2. Numerical studies of pre-impact, impact and post-impact phases for multi-arm open- and closed-loop impacts and investigating the effects of relative velocity and angle of approach on impact forces.

1.2.6 Summary

The impact modeling and estimation is taken up in this work for the multi-arm robotic systems for capture of tumbling objects. During the approach phase, the end effector of the space manipulator moves with a pre-defined trajectory which ensures zero relative velocity between end-effectors and grapple points during impact. However, it is very difficult to achieve the same in practice. When the object is tumbling, such soft approach might not exist. It may not be possible to grasp the object until its angular momentum decreases. During the impact phase, end-effector makes contact at a distinct point on the target object and impact forces are generated. These forces are modeled and estimated using conservation of momentum. The post impact phase is simulated by determining the change in generalized velocities of the end-effector and object during impact. The impact modeling of a multi-arm space robot forms the main contribution of this work.

Numerical illustrations are provided using a planar dual-arm robotic system where both arms are capturing two different objects in open-loop impact and same target object in closed-loop impact.

1.3 THESIS ORGANIZATION

The thesis contains five chapters which are organized as follows:

1. Introduction:

   The motivation and scope of the proposed research work are presented in this chapter. The important contributions and organization of the thesis are highlighted. Background and literature in the fields of impact modeling of multi-arm robotic systems have been critically reviewed in this chapter.

2. Kinematic and Dynamic Modeling of Multi-Arm Robot and Target:

   In this chapter basic formulation for a robotic system mounted on the satellite and the target object is presented. The dynamics of multi-arm robot has been presented for both open- and closed-loop systems. This formulation forms an essential framework in modeling the impact for multi-arm robot presented in Chapters 3.

3. Impact Model:

   In this chapter, a framework for impact modeling of pre-impact, impact and post-impact phases for a multi-arm floating base robot has been presented for capturing a tumbling orbiting object.

4. Results and Discussion:

   In this chapter, numerical illustrations are provided using a planar dual-arm robotic system capturing orbiting objects in different cases. The Post impact behaviour of the robot is also simulated along with study of effect of relative velocity and angle of approach on the impulsive forces.

5. Conclusions:

   This chapter gives the summary of the major results obtained in this research work, along with the conclusions. The scope of future work is also outlined in this chapter.

Appendix A: Kinematic Equations of Dual-arm space robot

Appendix B: Dynamical Equations of Dual-arm space robot

Appendix C: Momentum Conservation Equations

References

...

2

Kinematic and Dynamic Modeling of Multi-Arm Robot and Target

The robot kinematics is essential for describing an end-effector's position, orientation as well as motion of all the joints, while dynamics modeling is crucial for understanding the dynamic behavior of the robot. In this chapter, the kinematic and dynamic models of a multi-arm robot and a tumbling orbiting object are presented. When the multiple arms of robot capture different objects, then it acts as an open-loop system. On the other hand, when multiple arms capture the same object from different contact points, then it becomes a closed-loop system. Thus, the dynamics of robot has been presented for both open- and closed-loop systems. The target dynamics has been modeled considering it to be a rigid body.

2.1 KINEMATICS OF MULTI-ARM ROBOT

The multi-arm robotic system is mounted on a service satellite, which is assumed to be free-floating. The Jacobian that maps joint velocities into the end-effectors' velocities and incorporates motion of the base satellite need to be involved. Hence, the systematic derivation of the Jacobian for multi-arm space robot is presented in this section.

For the n-Degrees-of-freedom (DOF) multi-arm robotic system with r-end-effectors, as shown in Fig. 2.1, the end-effectors' velocities (t_{ei}) are expressed in terms of the base velocity and joint velocity as

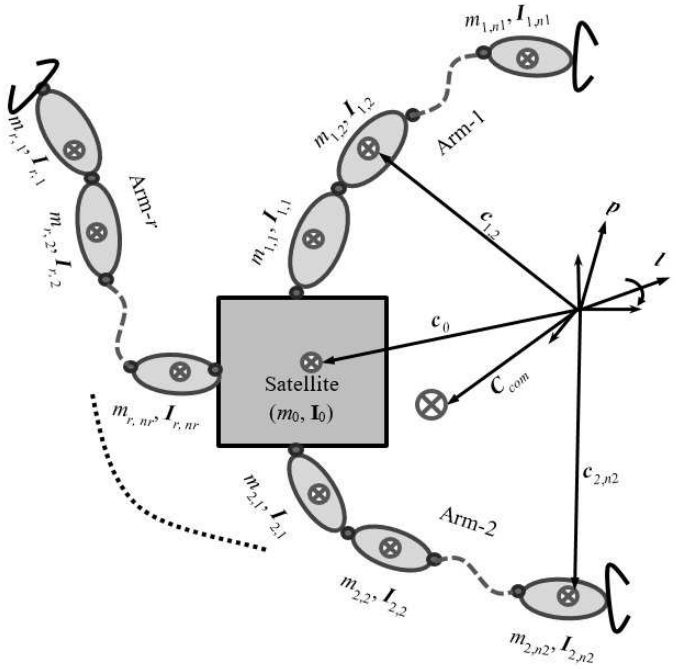

Figure 2.1. : A multi-arm robotic system mounted on a service satellite. The robot has r arms and the j_{th} arm has n_j links and n_j joints. Mass and inertia tensor of the k_{th} link on the j_{th} arm are denoted by $m_{j,k}$ and $I_{j,k}$, respectively. p and l are the linear and angular momenta, respectively. The total degree of freedom of the system is $n_1 + ... + n_r = n$

$$\begin{bmatrix} t_{e1} \\ \vdots \\ t_{er} \end{bmatrix} = \begin{bmatrix} J_{b1} \\ \vdots \\ J_{br} \end{bmatrix} t_b + \begin{bmatrix} J_{m1} & \dots & O \\ \vdots & \ddots & \vdots \\ O & \dots & J_{mr} \end{bmatrix} \begin{bmatrix} \dot{\theta}_1 \\ \vdots \\ \dot{\theta}_r \end{bmatrix} \tag{2.1}$$

Here, $t_b \in R^6$ is the twist constituting linear and angular velocities of the base. In addition, $\dot{\theta}_i \in R^{n_i}$ is the joint velocities vector of the i-th manipulator, $J_{bi} \in R^{6\times 6}$ is the Jacobian matrix from base to the end-effector of the i-th manipulator, and $J_{mi} \in R^{6\times n_i}$ is the Jacobian matrix for the i-th manipulator. Note that O is the null matrix of compatible dimensions.

One may note that end-effectors' velocities (t_{ei}) in (2.1) are represented in terms of both base velocities (t_b) and joint velocities ($\dot{\theta}_i$). In order to obtain Jacobian which maps $\dot{\theta}_i$ directly into t_{ei}, it is required to calculate t_b in terms of $\dot{\theta}_i$. This is obtained from the expressions of linear

momentum ($p \in R^{3\times1}$) and angular momentum ($l \in R^{3\times1}$) as an extension of dual-arm case presented in (Hafez et al., 2014), as

$$\begin{bmatrix} p \\ l \end{bmatrix} = I_b t_b + \sum_{i=1}^{r} I_{bmi}\dot{\theta}_i + \begin{bmatrix} 0 \\ c_0 \times p \end{bmatrix}. \tag{2.2}$$

Here, $I_b \in R^{6\times6}$ is the inertia matrix of the floating-base, $I_{bmi} \in R^{6\times n_i}$ is the coupling inertia matrices for the i-th arm and c_0 is position vector of center-of-mass. Substituting t_b from (2.2) into (2.1) one obtains

$$\begin{bmatrix} t_{e1} \\ \vdots \\ t_{er} \end{bmatrix} = \left(J_m - J_b I_b^{-1} I_{bm}\right) \begin{bmatrix} \dot{\theta}_1 \\ \vdots \\ \dot{\theta}_r \end{bmatrix} + J_b I_b^{-1} \begin{bmatrix} p \\ l - c_0 \times p \end{bmatrix} \tag{2.3}$$

$$J_b = \begin{bmatrix} J_{b1} \\ \vdots \\ J_{br} \end{bmatrix}, J_m = \begin{bmatrix} J_{m1} & \dots & O \\ \vdots & \ddots & \vdots \\ O & \dots & J_{mr} \end{bmatrix}, I_{bm} = \begin{bmatrix} I_{bm1} & \dots & I_{bmr} \end{bmatrix}.$$

where $J_b \in R^{6r\times6}$, $J_m \in R^{6r\times n}$ and $I_{bm} \in R^{6\times n}$. If no external force is acting on the base, and the system starts from rest, $p = l = 0$, and hence,

$$\begin{bmatrix} t_{e1} \\ \vdots \\ t_{er} \end{bmatrix} = \begin{bmatrix} J_{g,11} & \dots & J_{g,1r} \\ \vdots & \ddots & \vdots \\ J_{g,r1} & \dots & J_{g,rr} \end{bmatrix} \begin{bmatrix} \dot{\theta}_1 \\ \vdots \\ \dot{\theta}_r \end{bmatrix}, \tag{2.4}$$

where

$$J_{g,ii} = \left(J_{mi} - J_{bi} I_b^{-1} I_{bmi}\right),$$

$$J_{g,ij} = -J_{bi} I_b^{-1} I_{bmj}. \tag{2.5}$$

The term J_g is referred to as Generalized Jacobian Matrix (GJM) (Saha, 1996; Umetani and Yoshida, 1989) as mentioned. The GJM in (2.4) is different than the Jacobian of the earth-based manipulator as the former contains inertia terms. It will be used for impact modeling of the multi-arm space robot in the subsequent sections.

Having solution of $\dot{\theta}_i$, the motion of the base-satellite is obtained using (2.2) and substituting $P = L = 0$ as

$$t_b = -I_b^{-1} \sum_{i=1}^{r} I_{bmi}\dot{\theta}_i \tag{2.6}$$

2.2 DYNAMICS OF OPEN MULTI-ARM ROBOT

Multi-arm robot is said to be open-loop system if multiple arms capture multiple targets i.e. *r*-arms of a robot will capture *r*-targets. In this section, the Equations-of-Motion (EOM) for a multi-arm robot mounted on a service satellite is presented. Derivation of the EOM is referred to as dynamic modeling. In this thesis, DeNOC matrices have been used to obtain equations of motion for the free-floating robotic system. These DeNOC matrices when combined with the uncoupled NE equations of motion give rise to the minimal-order constrained dynamic equations of motion of the system at hand by eliminating the constraint forces.

The EOM for a multi-arm *n*-DOF robotic system mounted on a floating-base as shown in Fig. 2.1, is written as

$$\begin{bmatrix} I_b & I_{bm} \\ I_{bm}^T & I_m \end{bmatrix} \begin{bmatrix} \dot{t}_b \\ \ddot{\theta} \end{bmatrix} + \begin{bmatrix} c_b \\ c_m \end{bmatrix} = \begin{bmatrix} F_b \\ \tau_m \end{bmatrix} + \begin{bmatrix} J_{be}^T \\ J_{me}^T \end{bmatrix} F_e \tag{2.7}$$

where

$I_b \in R^{6\times 6}$ and $I_m = diag\begin{bmatrix} I_{m1} & \dots & I_{mi} & \dots & I_{mr} \end{bmatrix} \in R^{n\times n}$ are the inertia matrices of the base and manipulators, respectively,

$I_{bm} = \begin{bmatrix} I_{bm1} & \dots & I_{bmi} & \dots & I_{bmr} \end{bmatrix} \in R^{6\times n}$ is the coupling inertia matrix,

$\dot{t}_b = \begin{bmatrix} \dot{\omega}_b^T & \dot{v}_b^T \end{bmatrix}^T \in R^{6\times 1}$ is the vector of angular and linear accelerations of the base,

$\ddot{\theta} = \begin{bmatrix} \ddot{\theta}_1^T & \dots & \ddot{\theta}_i^T & \dots & \ddot{\theta}_r^T \end{bmatrix}^T \in R^{n\times 1}$ is the vector of joint accelerations,

$c_b \in R^{6\times 1}$ and $c_m = \begin{bmatrix} c_{m1}^T & \dots & c_{mi}^T & \dots & c_{mr}^T \end{bmatrix}^T \in R^{n\times 1}$ are the velocity dependent nonlinear terms associated with the base and manipulator, respectively,

$f_b \in R^{6\times 1}$ and $F_e \in R^{6r\times 1}$ are the vectors of moments and forces exerted on the centroid of base and end-effectors, respectively,

$\tau_m = \begin{bmatrix} \tau_{m1}^T & \dots & \tau_{mi}^T & \dots & \tau_{mr}^T \end{bmatrix}^T \in R^{n\times 1}$ is the vector of manipulator joint torques and

$J_{be} \in R^{6r\times 6}$and $J_{me} \in R^{6r\times n}$ are the Jacobian matrices for the base and manipulator, respectively.

It may be noted that I_{mi} is the inertia matrix, I_{bmi} is the coupling inertia matrix, c_{mi} is the velocity dependent non-linear term, τ_{mi} is the joint torque and $\ddot{\theta}_i = \begin{bmatrix} \ddot{\theta}_{1i} & \dots & \ddot{\theta}_{ki} & \dots & \ddot{\theta}_{ni} \end{bmatrix}^T$ is the vector of joint accelerations for the i^{th} arm.

The reduced form of the EOM of free-floating robot (Nenchev and Yoshida, 1999) would be used for modeling impact. The reduced form can be obtained by omitting base acceleration $\dot{\imath}_b$ from (2.7), as:

$$I\ddot{\theta} + c = \tau + J^T F_e \tag{2.8}$$

where $I = I_m - I_{bm}^T I_b^{-1} I_{bm}$ is the Generalized Inertia Matrix (GIM), $c = c_m - I_{bm}^T I_b^{-1} c_b$ is the Generalized Coriolis and centrifugal force, $\tau = \tau_m - I_{bm}^T I_b^{-1} F_b$ is the Generalized torque and $J^T = J_{me}^T - I_{bm}^T I_b^{-1} J_{be}^T$ is the Generalized Jacobian Matrix (GJM) (Saha, 1996; Umetani and Yoshida, 1989) for the free-floating robot.

2.3 DYNAMICS OF CLOSED MULTI-ARM ROBOT

The Multi-arm robot will become a closed-loop system if two or more arms will capture the same target objects from different contact points. In order to analyze a closed-loop system, it is first opened at appropriate joints to form a tree-type system. The opened joints are substituted with suitable constraint forces, λs, also known as Lagrange multipliers, which are then treated as external forces to the resulting open tree-type system. As a result, the problem is converted to a problem of tree-type system with externally applied constraint forces. Hence equations of motion can be represented as

$$I\ddot{\theta} + c = \tau + J^T F_e + J_c^T \lambda \tag{2.9}$$

where J_c is the constrained Jacobian matrix (Nikravesh, 1988) for the closed-loop system, and is defined in a way so that $J_c\dot{\theta} = 0$. Moreover, λ is the vector of Lagrange multipliers representing the constraint forces at the cut opened joints. There are several methods of solving (2.9) as shown by Shabana (2009). However, concept of "determinate" and "indeterminate" subsystems, as proposed

by Chaudhary and Saha (2008), has been proven to be more powerful and elegant approach in comparison with others for the dynamic analyses of closed-loop systems. Conventionally (Shabana, 2009) forward dynamics of closed-loop system solves independent accelerations ($\ddot{\theta}$) and constraint forces (λ) together by combining the equations of motion in (2.9), and the second order derivative of the constrained equations in the form of $J_c\ddot{\theta} = -\dot{J}_c\dot{\theta}$. They are shown as

$$\begin{bmatrix} I & J_c{}^T \\ J_c & 0 \end{bmatrix} \begin{bmatrix} \ddot{\theta} \\ -\lambda \end{bmatrix} = \begin{bmatrix} \phi \\ -\dot{J}_c\dot{\theta} \end{bmatrix}, \text{ where } \phi = \tau + J^T F_e - c \tag{2.10}$$

The formulation in (2.10) is popularly known as Differential Algebraic Equations (DAE) formulation. Alternatively, λ can be obtained first after rearranging (2.10) as

$$\lambda = -S_I^{-1}(J_c I^{-1}\phi + \dot{J}_c\dot{\theta}), \text{ where } S_I = J_c I^{-1} J_c^T \tag{2.11}$$

Next, the solution of the joint accelerations is obtained as

$$\ddot{\theta} = I^{-1}(J_c^T\lambda + \phi) \tag{2.12}$$

2.4 TARGET DYNAMICS

In this section, the EOM for a tumbling orbiting object is presented. It is assumed that at a given instant of time, r manipulators capture r objects. These objects are modeled as free-floating rigid bodies.

The EOM for r-targets can be written as:

$$I_t\dot{t}_t = \tau_t - J_t^T F_e \tag{2.13}$$

where $\tau_t \in R^{6r\times 1}$ is the vector of generalized moments and forces exerted on target object, $I_t \in R^{6r\times 6r}$ is the inertia matrix, $\dot{t}_t \in R^{6r\times 1}$ is the linear and angular acceleration vector and $J_t \in R^{6r\times 6r}$ is the Jacobian for r-objects. The I_t, $\dot{t}_t$ and J_t in case of r-targets can be written as:

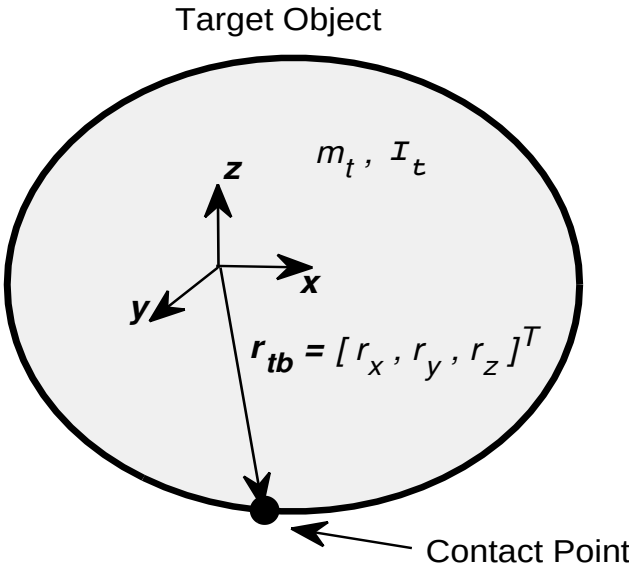

Figure 2.2. : A free-floating target object

$$
\begin{aligned}
I_t &= diag\begin{bmatrix} M_{t1} & \dots & M_{ti} & \dots & M_{tr} \end{bmatrix} \\
\dot{t}_t &= \begin{bmatrix} \dot{t}_{t1}^T & \dots & \dot{t}_{ti}^T & \dots & \dot{t}_{tr}^T \end{bmatrix}^T \\
J_t &= diag\begin{bmatrix} J_{t1} & \dots & J_{ti} & \dots & J_{tr} \end{bmatrix}
\end{aligned} \tag{2.14}
$$

where

$$
\begin{aligned}
M_{ti} &= \begin{bmatrix} I_t^c & O \\ O & m_t 1 \end{bmatrix}_i \\
\dot{t}_{ti} &= \begin{bmatrix} \dot{\omega}_t^T & \dot{v}_t^T \end{bmatrix}_i^T \\
J_{ti} &= \begin{bmatrix} 1 & O \\ R_{tb} & 1 \end{bmatrix}_i
\end{aligned} \tag{2.15}
$$

In (2.15), m_t is the mass and $I_t^c \in R^{3\times3}$ is the centroidal inertia tensor of the i^{th} object, $1 \in R^{3\times3}$ is identity matrix and O is the null matrix of compatible dimension. $\omega_t \in R^{3\times1}$ and $v_t \in R^{3\times1}$ are the angular and linear velocity vectors of i^{th} target, respectively. R_{tb} is the cross-product tensor associated with r_{tb}, which is the position vector from Centre-of-Mass (COM) of the i^{th} target to the point of contact as shown in Fig. 2.2.

2.5 AN ILLUSTRATION

For better understanding of the formulation presented in the above chapter, the kinematics and dynamics of multi-arm robot has been provided in the Appendices A and B, respectively. The dual-arm robot having 2-links on arm 1 and 1-link on arm 2, as shown in Fig. 2.3, is taken as an example. In kinematics, the jacobian matrix for base and manipulator in (2.1) have been presented. In dynamics, the EOM have been derived for the same system using DeNOC formulation.

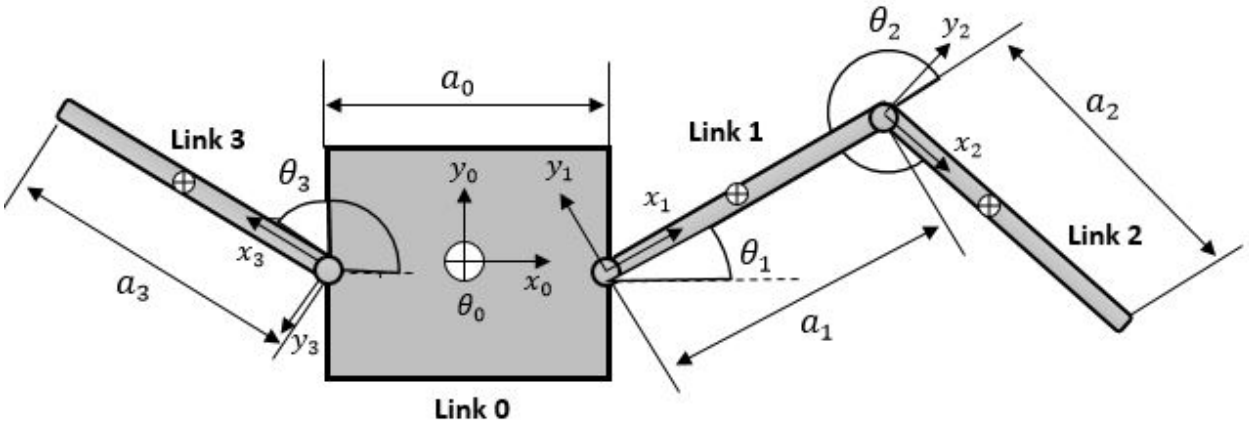

Figure 2.3. : Schematic diagram of multi-arm space robot

The equations are also presented in matrix form to have a better understanding of the general form of EOM of multi-arm robot presented in (2.7). Also the momentum conservation equations in (2.2) have been presented in Appendix C. These equations have been used extensively in impact modeling of multi-arm robot.

...

3
Impact Model

The objective of impact modeling is to determine the post impact conditions of the system, given its initial (pre-impact) configuration. Impact is a complex phenomenon that occurs when two or more bodies undergo a collision. In this chapter, the mathematical model of the impact of multi-arm robot with orbiting object is presented. The impact is considered to be inelastic i.e. the orbiting object will become rigidly attached to the space robot after impact. In normal applications, impact takes place because of the velocity of the end effector relative to the object at the time of contact, which effects the velocities and internal forces of the robotic system. First, the generalized velocities representing joint rates having abrupt changes at the moment of impact with the object are determined. The mathematical model is derived to establish the quantitative relationship between this abrupt change and the severity of the impact. Later the formulation has been given to estimate impulse due to impact.

The following assumptions are made while modeling impact dynamics of the multi-arm space robot:

1. The time duration of impact is so short (approximately 10^{-3} s) that the generalized position coordinates of the system remain same over the impact duration, while the generalized velocities change substantially.

2. The effect of other forces except the impact force can be disregarded. From this assumption, we can say that the inertia term of dynamic equation is dominant and other terms are less important for the system dynamics at impact.

3.1 PRE-IMPACT PHASE

In order to capture the target, the end-effector has to move from its initial pose (position and orientation) to the capture point. In the case of tumbling target, the end-effector begins with zero velocity and approaches with the prescribed final velocity. For this the independent joint velocities are designed using a fourth order interpolating polynomial as follows:

$$\dot{\theta}_k(t) = \frac{\theta_k(T) - \theta_k(0)}{T}\left[a\left(\frac{t}{T}\right)^2 + b\left(\frac{t}{T}\right)^3 + c\left(\frac{t}{T}\right)^4\right] \tag{3.1}$$

where

$$a = 3(-4s+10),\ b = 4(7s-15),\ c = 5(-3s+6)$$

$$s = \frac{\dot{\theta}_k(T)}{\frac{\theta_k(T)-\theta_k(0)}{T}} \tag{3.2}$$

The above trajectory ensures zero initial velocity and acceleration and zero final acceleration, whereas final velocity is $\dot{\theta}_k(T)$ for the k^{th} joint on i^{th} arm. The trajectory requires initial $\theta_k(0)$ and final $\theta_k(T)$ positions as the inputs.

3.2 IMPACT PHASE

The Impact modeling for 2-link robot has already been proposed in (Cyril et al., 1993). This model has been extended for impact modeling of multi-arm space robot with one or more target objects. To model the impact phase, let us consider that the target object collides with the end effector of the robot arm mounted on a service satellite at a known single point and as a result of this collision, impact force F_e is induced.

By combining (2.8) and (2.13), the impact force F_e can be eliminated to obtain the following equation:

$$J^T J_t^{-T} I_t \dot{i}_t + I\ddot{\theta} = -c\ +\ \tau + J^T J_t^{-T} \tau_t \tag{3.3}$$

Let the duration of impact be T seconds. Now (3.3) would be integrated over T time period.

Before integrating, one can recall the assumption (1) that all of the generalized position coordinates of the system remain same over this period, although the generalized velocities and accelerations may change. Since J, J_t, I_t, I depend only on the position coordinates, these matrices would remain constant and thus can be taken out of the integral. Also, the impact force is usually very large and acts for a very short time T. Thus one can say that (Cyril et al., 1993)

$$T = O(\varepsilon), \quad where \quad \varepsilon << 1$$

$$\dot{\theta}, t_t = O(1)$$

$$\ddot{\theta}, \dot{t}_t = O(1/\varepsilon) \tag{3.4}$$

Now, integration of (3.3) over time period T would give:

$$J^T J_t^{-T} I_t (t_{tf} - t_{ti}) + I(\dot{\theta}_f - \dot{\theta}_i) = \int_0^T [-c \ + \ \tau + J^T J_t^{-T} \tau_t] dt \tag{3.5}$$

where the subscripts f and i stand for values after and before the impact, respectively. Clearly, the left-hand side of (3.5) is $O(1)$. The integrand on the right-hand side is also $O(1)$; however, the interval of the integration is of $O(\varepsilon)$ and, hence, the right-hand side is of $O(\varepsilon)$ and can be ignored compared to the left-hand side. Thus (3.5) can be written as

$$J^T J_t^{-T} I_t (t_{tf} - t_{ti}) + I(\dot{\theta}_f - \dot{\theta}_i) = 0 \tag{3.6}$$

The above equation represents conservation of generalized momenta and is valid for all collisions.

3.2.1 Impact Force Estimation

The impact force estimation is very important part of impact modeling. This force calculation would help in designing the prototype or physical system for conducting the experiments. To calculate the magnitude of impulse $\overline{F}$ during impact, F_e from (2.8) and (2.13) is rearranged to give following expression.

$$F_e = J^{-T}(I\ddot{\theta} - c - \tau)$$

$$F_e = -J_t^{-T}(I_t \dot{t}_t - \tau) \tag{3.7}$$

The (3.7) is then integrated over time duration of impact T to give magnitude of impulse as

$$\overline{F} = J^{-T} I(\dot{\theta}_f - \dot{\theta}_i) \tag{3.8}$$

The $\overline{F}$ vector gives both linear and angular impulse. The impact force can then be calculated by multiplying the magnitude of linear impulse force with time duration of impact.

3.3 POST-IMPACT PHASE

The post impact dynamics depends on the fact that the impact is inelastic or elastic. In case of inelastic impact, the two systems become rigidly attached to each other after impact at the contact points, whereas in the case of elastic impact, the systems rebound with no loss of energy. In this paper, the impact is assumed to be inelastic and is modeled for capturing and berthing operations.

3.3.1 Velocity Estimation

In plastic impact, the velocity of end effector and contact point would be same, i.e.,

$$J\dot{\theta}_f = J_t t_{tf} \tag{3.9}$$

The generalized velocities of the target can be written in terms of manipulator velocities to get

$$t_{tf} = J_t^{-1} J\dot{\theta}_f \tag{3.10}$$

Substitution of (3.10) into (3.6) yields

$$\dot{\theta}_f = G^{-1} H \tag{3.11}$$

where

$$G = J^T J_t^{-T} I_t J_t^{-1} J + I$$

$$H = J^T J_t^{-T} I_t t_{ti} + I\dot{\theta}_i \tag{3.12}$$

From (3.11) we can obtain final velocities for space robot, which can be used to calculate change in target velocities using (3.10). The final base velocities $\dot{i}_{bf}$ can be obtained using the momentum

equation (Gattupalli et al., 2013) as given by

$$\dot{t}_{bf} = I_b^{-1}\left(\begin{bmatrix} p \\ l - c_o \times p \end{bmatrix} - I_{bm}\dot{\theta}_f \right) \tag{3.13}$$

The detailed derivation of this momentum equation is given in Appendix C. From (3.11) and (3.13) we get generalized velocity vector as an initial condition for the post impact dynamic simulations.

...

4
Results and Discussion

In this chapter the proposed frame-work has been implemented on the multi-arm space robot, while capturing orbiting tumbling object. A 3-link dual arm robot mounted on a service satellite has been choosen as an example for performing numerical experiments. The solid sphere rotating about its z-axis has been considered as a target object. The schematic diagram of multi arm robot and the target object is shown in Fig. 4.1.

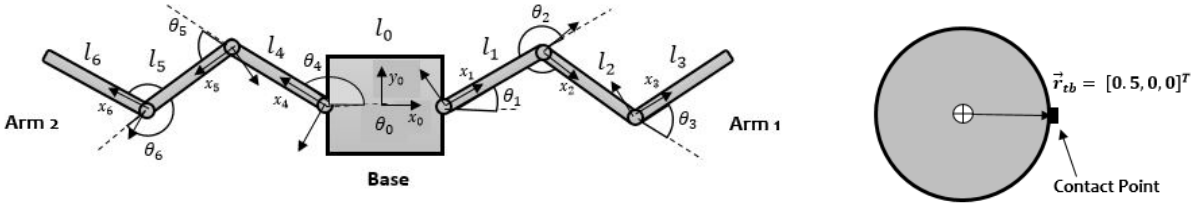

$$\theta_{e1} = \theta_0 + \theta_1 + \theta_2 + \theta_3,\ \theta_{e2} = \theta_0 + \theta_4 + \theta_5 + \theta_6$$

Figure 4.1. : Schematic diagram of multi-arm robot and target

The link length, mass and inertia properties of the base and robot, used for the purpose of simulation, are provided in Table 4.1. The mass and mass Moment of Inertia (MOI) of target objects are given in Table 4.2. The COM of the satellite is located at $(0,0)$, while the location of two target objects in the XY-plane are given in Table 4.2. The numerical experiments are performed on both open- and closed-loop systems. The capability of Recursive Dynamics Simulator (ReDySim) (Shah et al., 2012b), which is a MATLAB based dynamic simulator, has been enhanced and consequently used for the purpose of dynamic simulations in the pre-impact and post-impact phase for open- and closed-loop impact.

Table 4.1. : Model parameters of dual-arm robot and base

	Base	Robot					
		Arm 1			Arm 2		
Link	0	1	2	3	4	5	6
Length (m)	1	1	1	1	1	1	1
Mass (kg)	500	10	10	10	10	10	10
MOI (kg-m^2)	83.61	1.05	1.05	1.05	1.05	1.05	1.05

Table 4.2. : Model parameters of target

	Target 1	Target 2
Mass (kg)	10	10
Radius (m)	0.5	0.5
MOI (kg-m^2)	1	1
Location (m)	(2,-2)	(-2,2)

4.1 OPEN LOOP IMPACT

When both arms of a robot will capture two different target objects, then it is referred to as an open-loop impact. In the numerical experiments, three phases of impact are modeled and the behaviour of the system undergoing impact is estimated. In the approach phase, the trajectory in (3.1) is used so that the end-effector will have prescribed velocity at the point of contact. (3.1) requires initial and final joint angles as the inputs, which are given in Table 4.3. These initial and final joint angles are obtained from the end-effectors' final position as given in table 4.4 using inverse kinematics relationships. The initial joint velocities are taken as zero for all the joints. Also, the base of the satellite has zero linear and angular velocity as an initial condition. The initial and final positions for both end-effectors are given in Table 4.4. P_{e1x} and P_{e1y} are positions of end-effector

Table 4.3. : Desired initial and final joint angles

	Arm 1			Arm 2		
	θ_1	θ_2	θ_3	θ_4	θ_5	θ_6
Initial	0.698	-1.571	1.047	2.444	1.571	-1.047
Final	-0.524	-1.393	-0.035	2.618	-1.393	-0.035

1 in X and Y direction, respectively. Similarly, P_{e2x} and P_{e2y} are positions of end-effector 2. The

Table 4.4. : Initial and final end-effectors' position

	P_{e1x}	P_{e1y}	P_{e2x}	P_{e2y}
Initial	2.9	0.05	-2.9	0.05
Final	2	-1.5	-2	1.5

final position will be the point of contact on the surface of the target object. Moreover (3.1) also requires final joint velocities, which ensures zero relative velocity between end-effectors and grapple points during impact. Since both targets in Case 1 are assumed to have an angular velocity of 0.2 rad/s in anti-clockwise direction, so the linear velocity at the point of contact for a target object of 0.5 m radius would be 0.1 m/s. Thus, the end-effectors' velocities are taken as 0.1 m/s in -X directions for end-effector 1 and in +X direction for end-efffector 2. The respective joint velocities can be obtained using the GJM. The pre-impact simulations were carried out using ReDySim for the time period of 20s. The pre-impact and impact phase simulation results are shown in Figs. 4.2 and 4.3.

The trajectory following Proportional and Derivative (PD) control law at position level given by 4.1 was used for carrying out dynamic simulations.

$$\tau = K_p(\theta_d - \theta) + K_d(\dot{\theta}_d - \dot{\theta}) \tag{4.1}$$

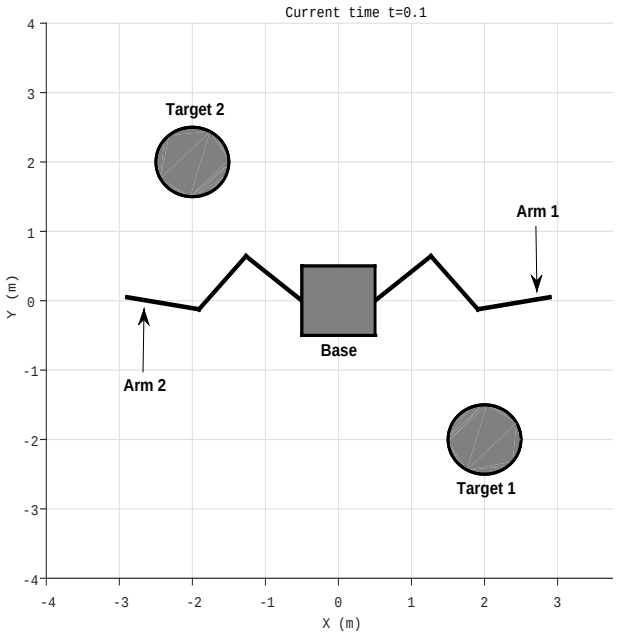

Figure 4.2. : Pre-impact initial configuration

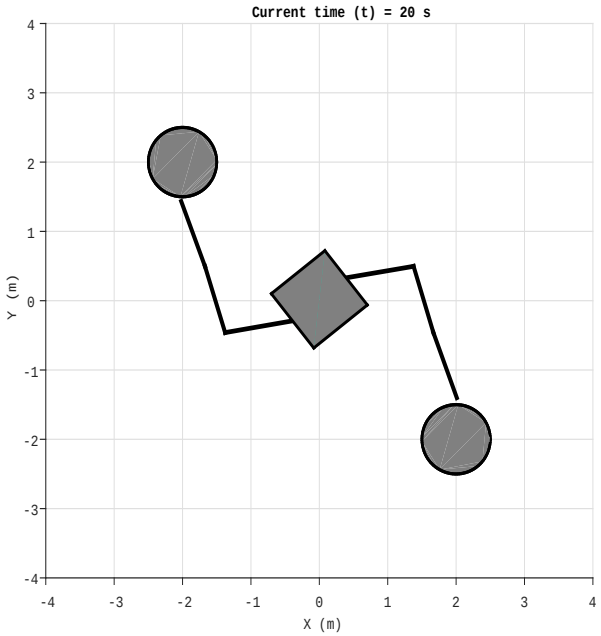

Figure 4.3. : Impact phase configuration

where, K_p and K_d are the diagonal matrices of proportional and derivative gains and $\dot{\theta}_d$ and $\dot{\theta}$ are desired and actual joint velocities, respectively. The values of K_p and K_d are taken as 49 and 14, respectively. The joints angles and end-effector's velocities achieved during forward dynamics simulation in approach phase are shown in Fig. 4.4 and Fig. 4.5, respectively. V_{e1x} and V_{e2x} is the linear velocity of the end-effector 1 in X and Y direction, respectively. Similarly, V_{e2x} and V_{e2y} is the linear velocity of the end-effector 2 in X and Y direction, respectively. It is evident from Fig. 4.5 that end-effector won't be able to reach prescribed velocity of 0.1 m/s. The velocity conditions at the time of impact are clearly shown in the Fig. 4.6. This velocity difference between the end-effector and point of contact on target object would cause an impact.

Since collision between robot arms and a target object is assumed as an inelastic case, therefore the momentum of the system should remain conserved before and after impact. Thus the total momentum of the system needs to be measured. For case 1, the total momentum of the robot and two target objects before impact is shown in Fig. 4.7.

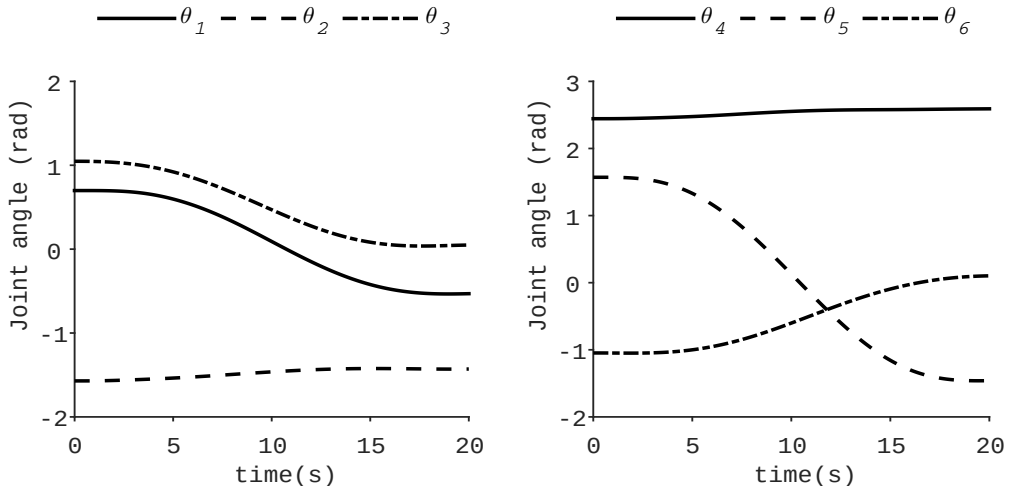

Figure 4.4. : Actual joint angles

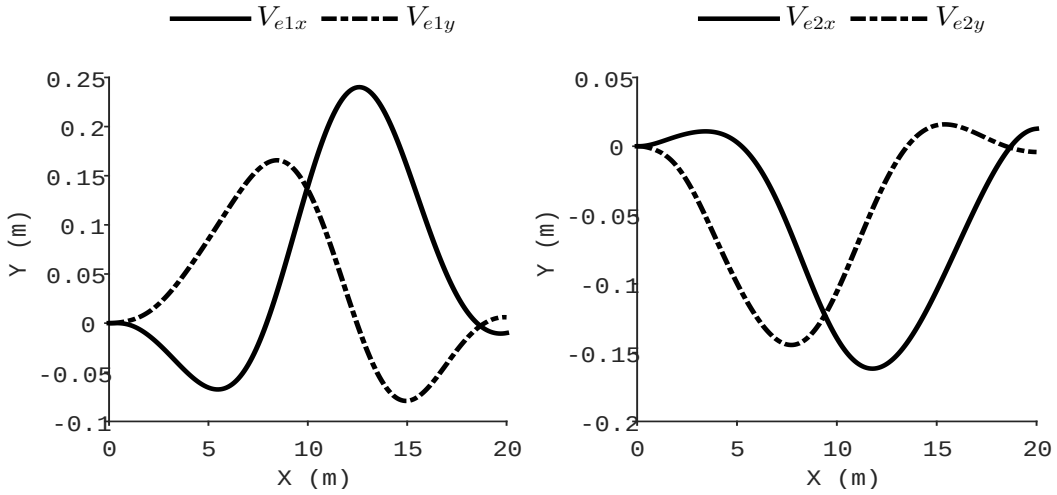

Figure 4.5. : End-effector velocity

In the Impact phase, (3.9) - (3.13) were used to model impact and estimate the change in velocities of the robot and target. The generalized velocity vector so obtained was used as an initial condition for post dynamic simulations. Since we assumed that the target is captured rigidly by the end effector as a perfectly inelastic case, so the robot and the target would become one system in post-impact phase. The post-impact simulations were also carried out using ReDySim for time-

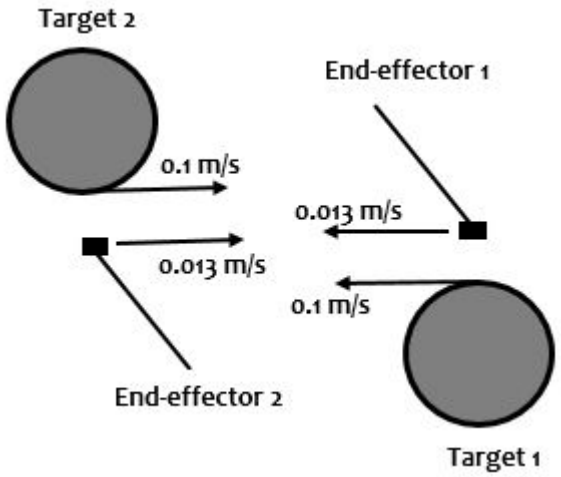

Figure 4.6. : Impact phase velocities

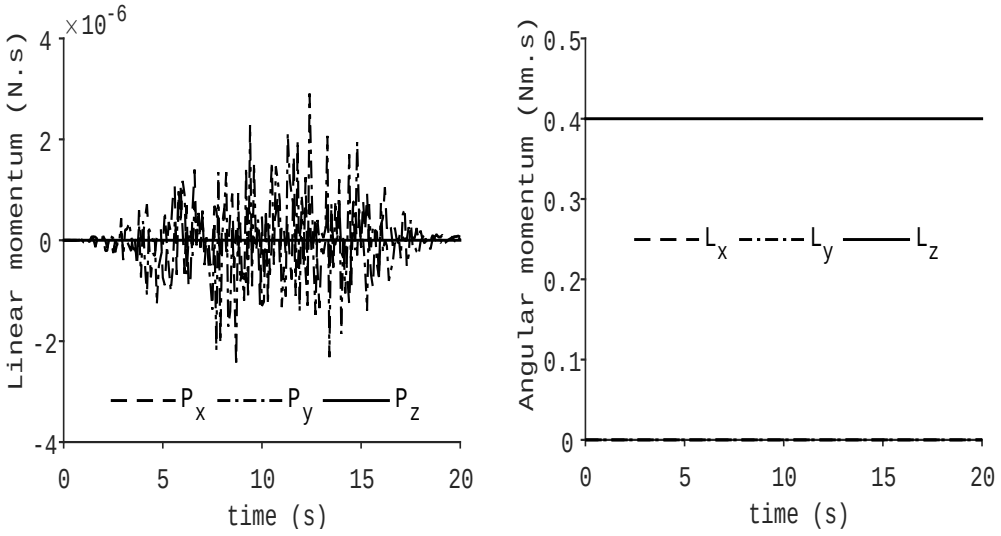

Figure 4.7. : Total momentum before impact

period of 50s. The following cases have been studied to validate our framework for post-impact dynamics:

Case 1 : **Both targets rotating in same direction**

In this case, target 1 and 2 are rotating in anticlockwise direction with an angular velocities of 0.2 rad/sec. The other initial conditions have already been discussed for this case. The post impact

dynamic behaviour of the system for this case is shown in Fig. 4.8. It has been observed that both arms kept on rotating in anticlockwise direction for a period of 50 sec.

Case 2 : **Both targets Stationary**

In this case, both targets are at rest. The simulation is shown in Fig. 4.9. Though the end-effectors' velocities are designed to achieve zero velocity at the point of contact but we will not be able to achieve the same. Due to this small velocity difference between end-effector and contact point, the system will undergo impact and as a result the small amount of arm movement has been observed.

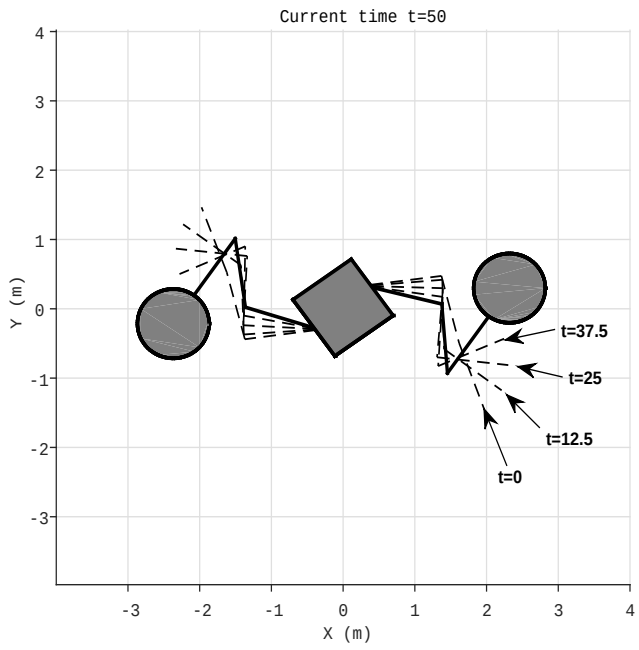

Figure 4.8. : Both target rotating CCW

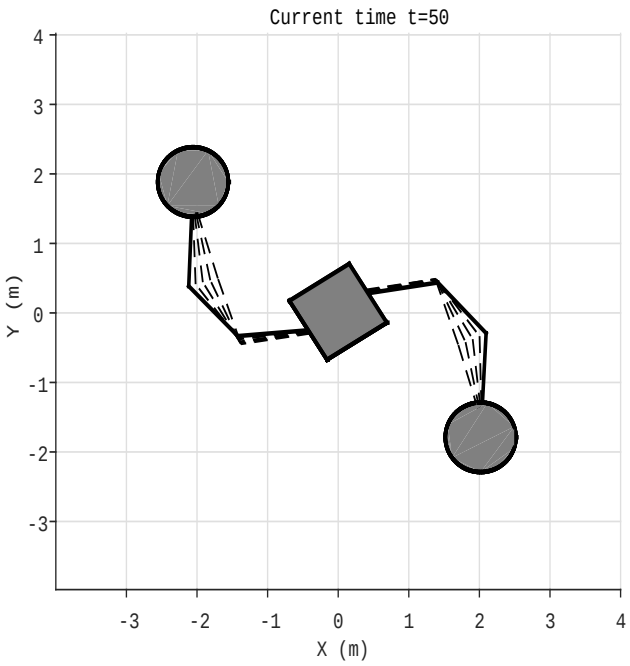

Figure 4.9. : Both target stationary

Case 3 : **Both targets rotating in opposite direction**

In this case, Target 1 is rotating in anticlockwise direction and Target 2 is rotating in clockwise direction. The target 1 and 2 has an angular velocity of 0.2 rad/sec and -0.2 rad/sec respectively. Thus end-effector 1 and 2 should have a linear velocity of 0.1 m/s in -X direction. Again due to

relative velocity between end-efffector and point of contact, the impact will occur . As a result the arms will undergo rotation in respective directions of target angular velocity. The Fig. 4.10 shows that the arm 1 will rotate in anti-clockwise direction as target 1 is rotating anticlockwise. Similarly arm 2 will undergo clockwise motion as target 2 is rotating clockwise.

Case 4 : **Target 1 stationary and target 2 rotating**

In this case, Target 1 is stationary and Target 2 is rotating in anticlockwise direction. The target 2 has an angular velocity of 0.2 rad/sec. Thus end-effector 2 should have a linear velocity of 0.1 m/s in -X direction. The post-impact dynamic simulation is shown in Fig. 4.11. It shows that the arm 1 will undergo small motion as target 1 is stationary, whereas arm 2 will undergo the anti-clockwise motion.

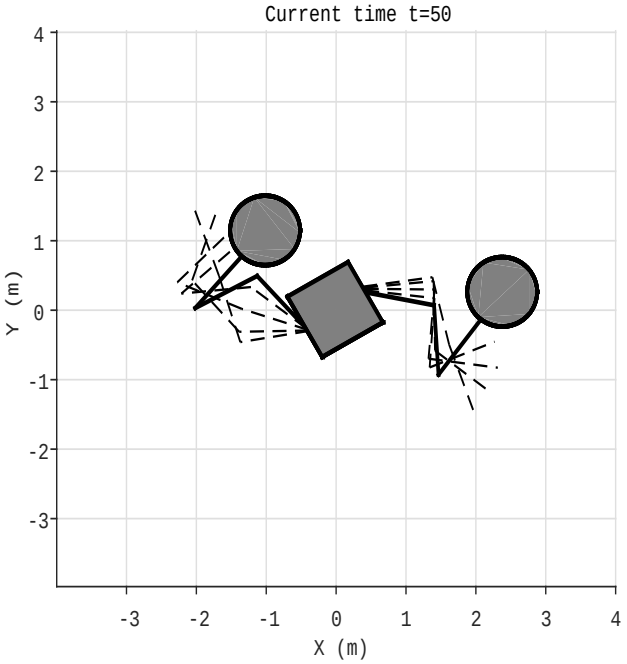

Figure 4.10. : Target 1 rotating CCW and target 2 CW

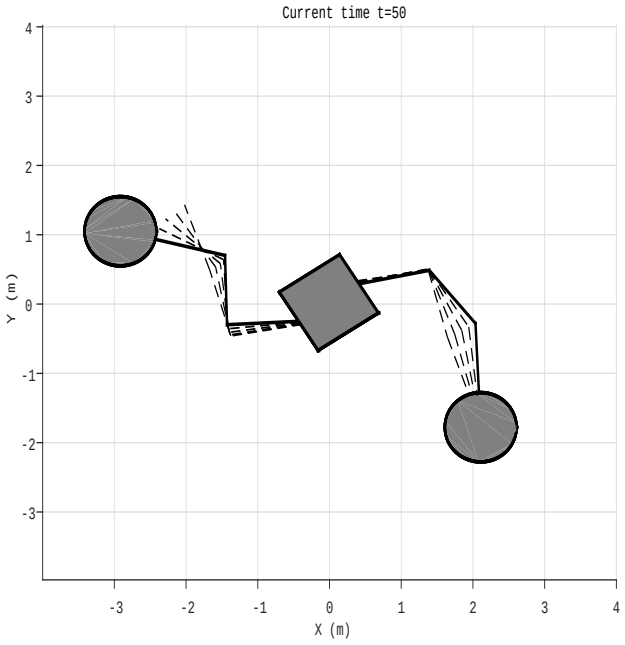

Figure 4.11. : One target stationary

From the above 4 cases, we can conclude that the proposed framework has been able to model impact and post-impact dynamics. Further to validate inelastic case of collision, we have calculated the total momentum of the system after impact in Case 1, as shown in Fig. 4.12. It is

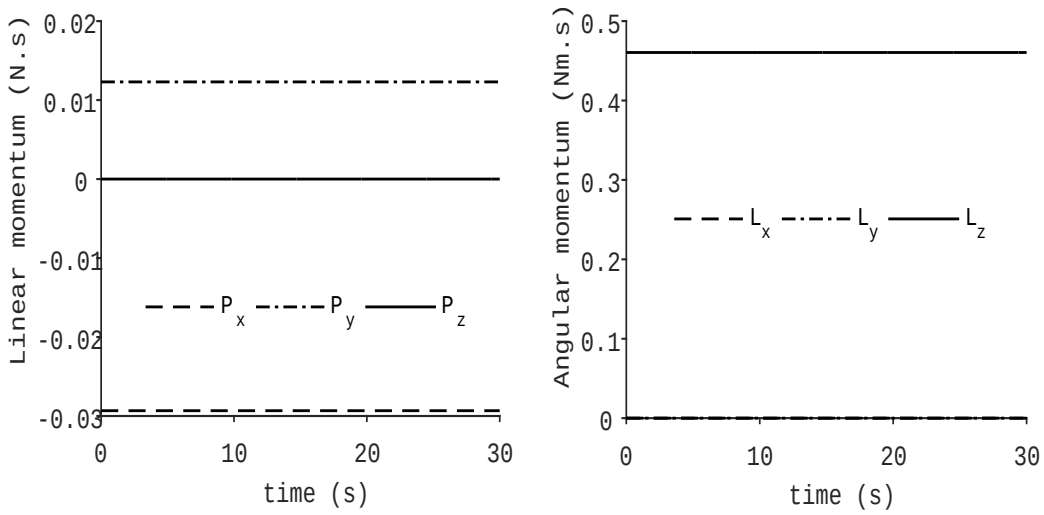

Figure 4.12. : Total momentum after impact

evident from the Figs. 4.7 and 4.12 that total momentum of the system is almost same before and after impact. Thus the laws of inelastic collision are verified which says that the total momentum of the system should remain conserved. Thus we can say that the proposed framework can correctly model inelastic impact for multi-arm robot.

4.2 CLOSED LOOP IMAPCT

When both arms of a robot will capture one target object from different points of contact, then it is termed as closed-loop impact. In the approach phase, the trajectory in (3.1) is used so that the end-effector will have prescribed velocity at the point of contact. (3.1) requires initial and final joint angles as the inputs, which are given in Table 4.5. These initial and final joint angles are obtained from the end-effectors' final position as given in table 4.4 using inverse kinematics relationships. The initial joint velocities are taken as zero for all the joints. Also, the base of the satellite has zero linear and angular velocity as an initial condition. The initial and final positions for both end-effectors are given in Table 4.6. The final position will be the point of contact on the surface of the target object. Moreover (3.1) also requires final joint velocities, which ensures zero

Table 4.5. : Desired initial and final joint angles

	Arm 1			Arm 2		
	θ_1	θ_2	θ_3	θ_4	θ_5	θ_6
Initial	0.785	-1.571	1.571	2.356	1.571	-1.571
Final	0.360	1.676	1.037	2.784	-1.583	-1.187

Table 4.6. : Initial and final end-effectors' position

	P_{e1x}	P_{e1y}	P_{e2x}	P_{e2y}
Initial	2.3	0.35	-2.3	0.35
Final	0.5	1.35	-0.5	1.35

relative velocity between end-effectors and grapple points during impact. Since target is assumed to have an angular velocity of 0.2 rad/s in anti-clockwise direction, so the linear velocity at the point of contact for a target object of 0.5 m radius would be 0.1 m/s. Thus, the end-effectors' velocities are taken as 0.1 m/s in +Y directions for end-effector 1 and in -Y direction for end-efffector 2. The respective joint velocities can be obtained using the GJM. The pre-impact simulations were carried out using ReDySim for the time period of 20s. The initial and final configuration of a robot while capturing one target object is shown in the Fig. 4.13 and 4.14, respectively. It is evident from the Fig. 4.14 that the system need to be simulated as closed-loop system in post impact phase when both arms capture a single target object. In the impact phase, (3.9) - (3.13) were used to model impact and estimate the change in velocities of the robot and target. The generalized velocity vector so obtained was used as an initial condition for post dynamic simulations. Since we assumed that the target is captured rigidly by the end effector as a perfectly inelastic case, so the robot and the target would become one system in post-impact phase. The System will not be subjected

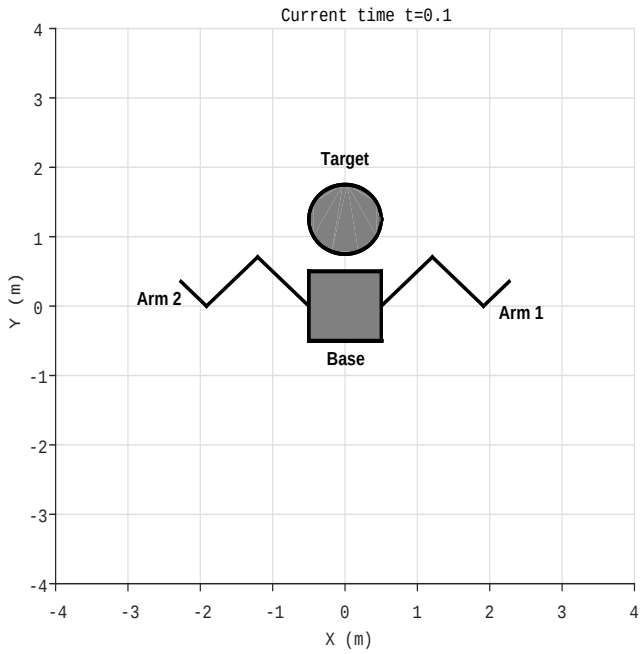

Figure 4.13. : Pre-impact initial configuration

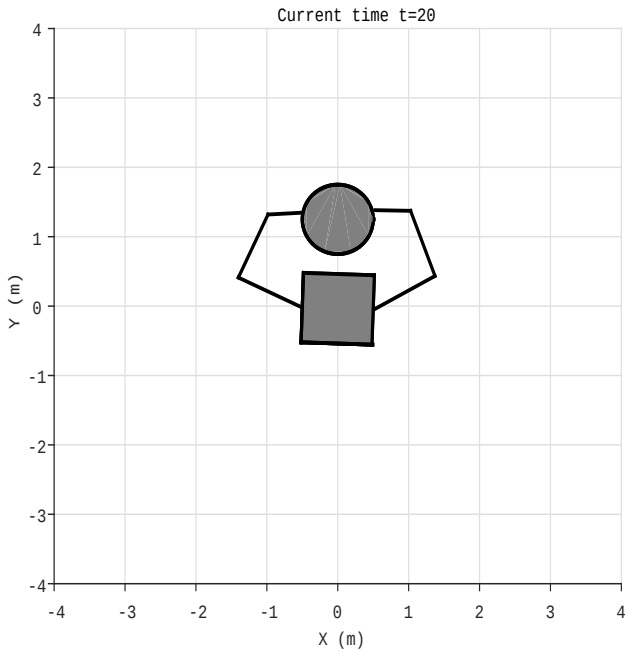

Figure 4.14. : Impact phase configuration

to any torque control law. The post impact simulations were also carried out using ReDySim for time-period of 50s. The Post impact dynamics simulation for closed loop is shown in Fig. 4.15. It is evident from Fig. 4.15 that system is not able to maintain closed loop in post impact phase, i.e. there is violation of constraint in a closed loop system in post impact phase. This may be due to the inappropriate velocities being supplied to the system. For closed loop systems, independent and dependent joint velocities need to be supplied accordingly so that closed loop constraint is not violated. Further study will be done in the future to simulate the closed loop impact of multi-arm robot.

We have also studied the loop closure violation, i.e. magnitude of the distance between the end of two open links, as shown in Fig. 4.16. This can be helpful to apply any stabilization technique so that the constraints will be satisfied and closed loop is maintained in the post impact phase.

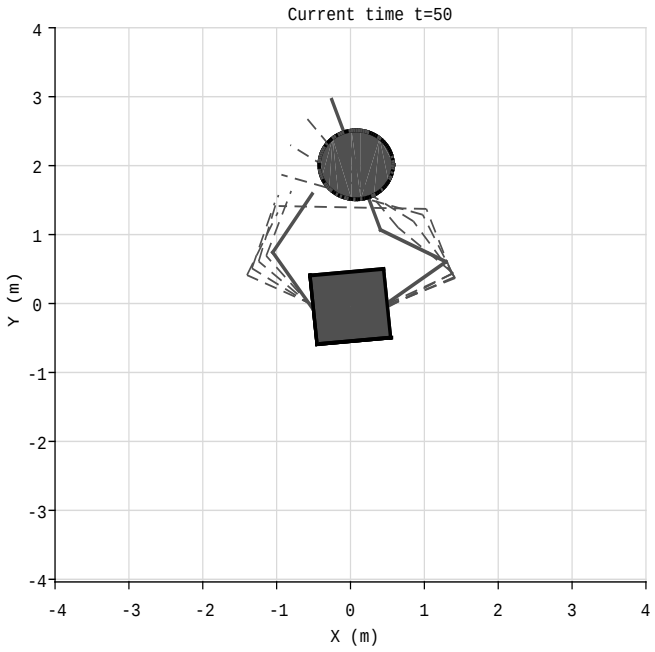

Figure 4.15. : Post impact dynamics

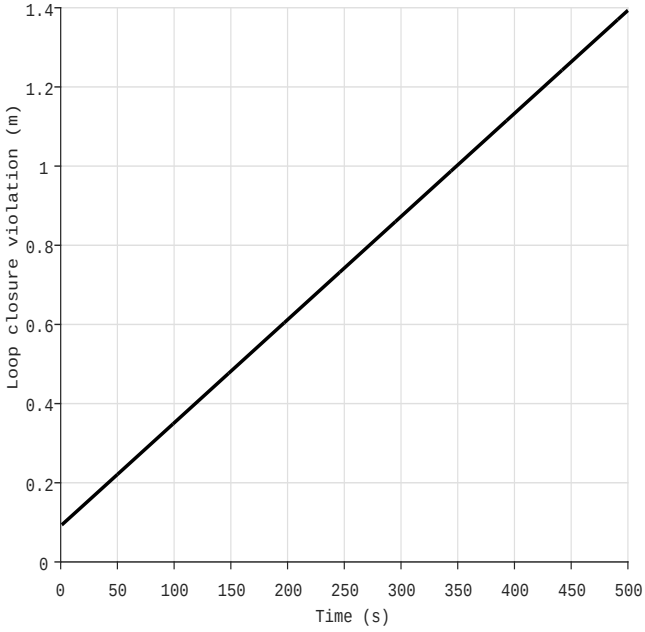

Figure 4.16. : Loop closure violation

4.3 IMPACT INVESTIGATION

The impact investigations have been done in this thesis, which would be very helpful for designing and simulating any such system. The various investigations include estimation of impulse forces at the time of impact. The magnitude of these forces can prove to be very helpful for designing multi-arm robot for capturing operations. The magnitude of the impulse is calculated using (3.8) and shown in Table 4.7 for all the 4 cases discussed above. The impact force can then be calculated by dividing impulse with time duration of the impact. It is evident from Table 4.7 that the magnitude of the impulse is less in case of stationary target (case 2) as compared to rotating target (case 1). The impact force has been experienced by the multi-arm robot in case of stationary target due to the existing velocity difference between end-effector and target contact point. The velocity difference affects the magnitude of impact forces, which is also investigated in this thesis.

In the approach phase, it is very essential that at the time of interception the velocity of the end-effector should be equal to that of a point to be grasped in order to avoid any impact. But

Table 4.7. : Impulse (N-s) estimation

Case	Impulse ($\overline{F}$)	
	Contact Point 1	Contact Point 2
Case 1	0.0873	0.0873
Case 2	0.0131	0.0131
Case 3	0.0873	0.0873
Case 4	0.0131	0.0873

in practice, there will be a nonzero relative velocity between the end-effector and the grapple point, leading to an impact. The magnitude of impact forces varies with that of relative velocities. So the investigation has been done to study the variation of impact forces with the magnitude of relative velocity. This variation has been observed for different motion of orbiting objects as described in the above 4 cases. It has also been found that the orientation of the end-effector (θ_e) i.e. angle of approach may affect the magnitude of impulse forces. Thus impulse forces have been studied for different angles of approach and different relative velocities. The Fig. 4.17 shows the three different end-effector orientation considered for studying impulse at the time of impact. The variation of

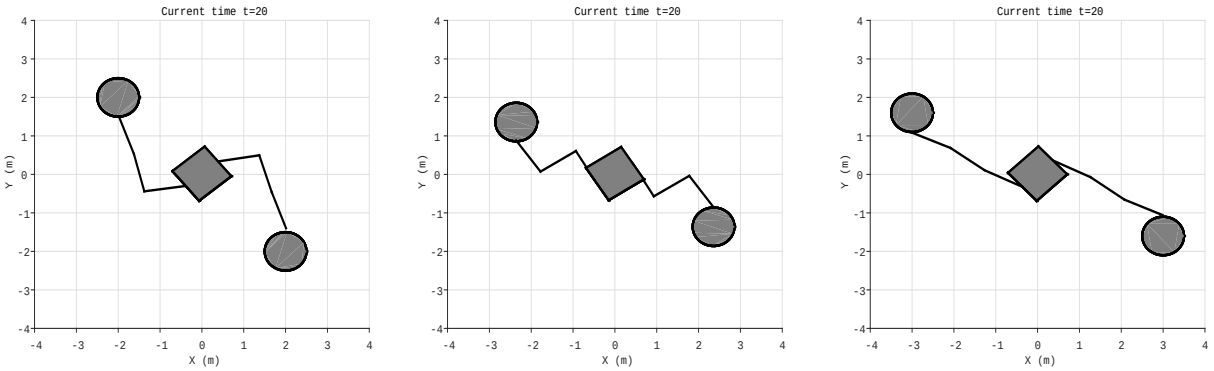

$\theta_e = 248^\circ$ $\theta_e = 269^\circ$ $\theta_e = 289^\circ$

Figure 4.17. : Different angles of approach in open-loop systems

magnitude of impulse with different relative velocities and angles of approach for open-loop systems

is shown in Fig. 4.18.

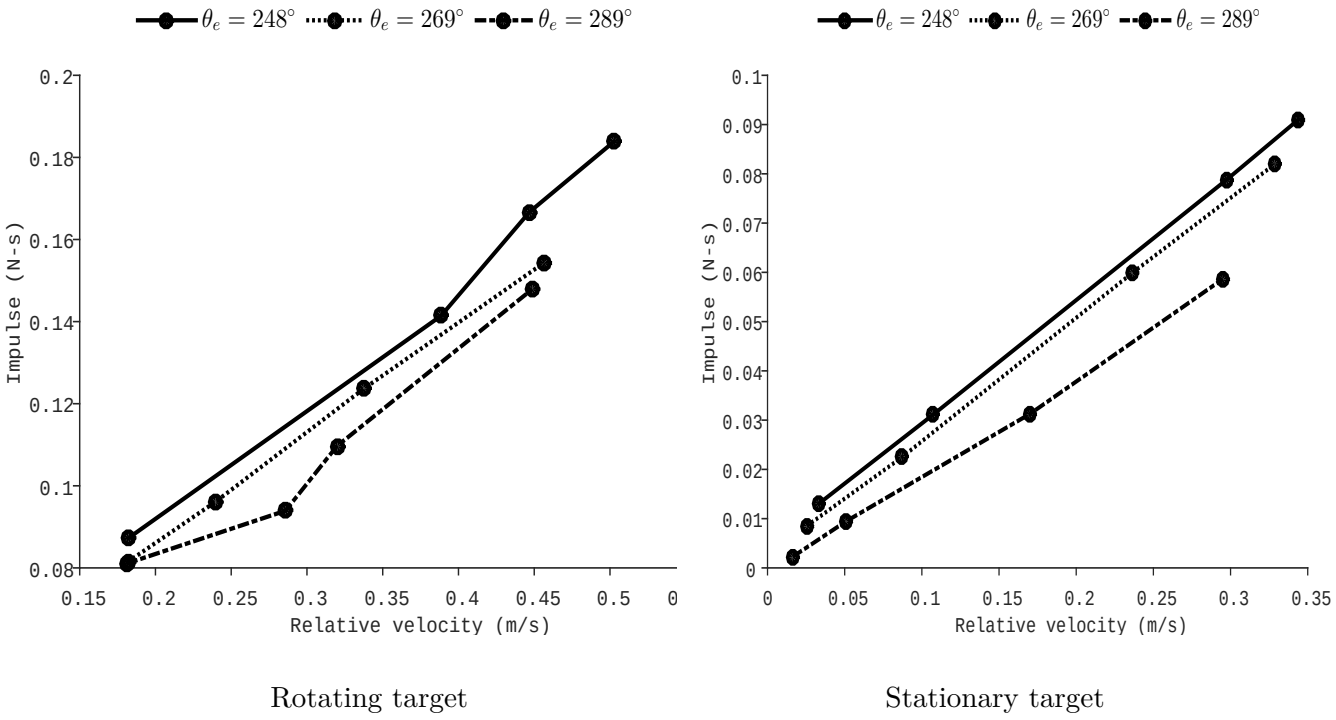

Rotating target Stationary target

Figure 4.18. : Impulse in open-loop systems

From Fig. 4.18, it has been observed that there is a linear relationship between magnitude of relative velocity and impulse, i.e. magnitude of impulse increases with increase in magnitude of relative velocity. Thus to minimize impact, there should be the least velocity difference between the end-effector velocity and target contact point. This is very difficult to achieve in practice. Thus controller should be designed with an objective to attain the minimum possible velocity difference. This could be helpful in minimizing impulsive forces. Also, it has been found that magnitude of impulse changes with the angle of approach. Thus, proper care should be taken while deciding end-effector pose for capturing orbiting object.

The impulse was also investigated for closed-loop systems. The same target with different motions as in open-loop systems has been observed. The impulse forces have been studied for different angle of approach and different relative velocities. The Fig. 4.19 shows the three different

angles of approach considered for studying impulse at the time of impact. The variation of impulse

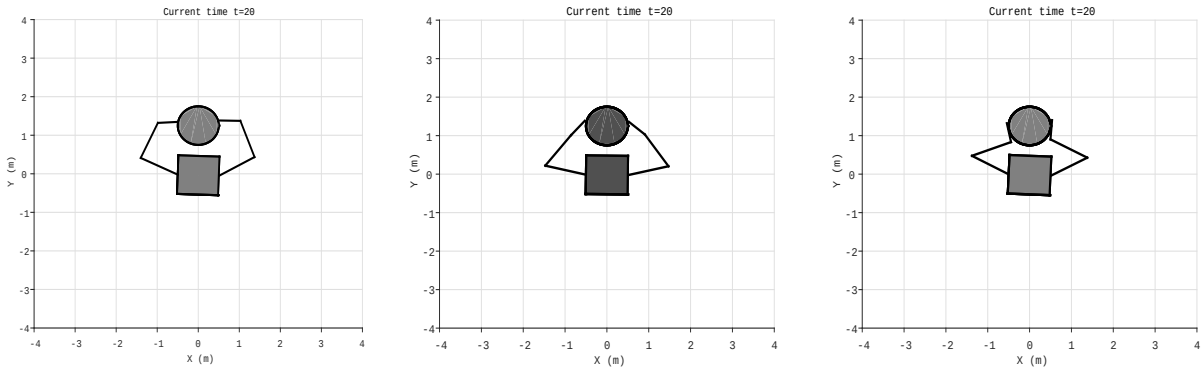

$\theta_e = 175°$ $\theta_e = 135°$ $\theta_e = 443°$

Figure 4.19. : Different angles of approach in closed-loop systems

with relative velocity is shown in Fig. 4.20.

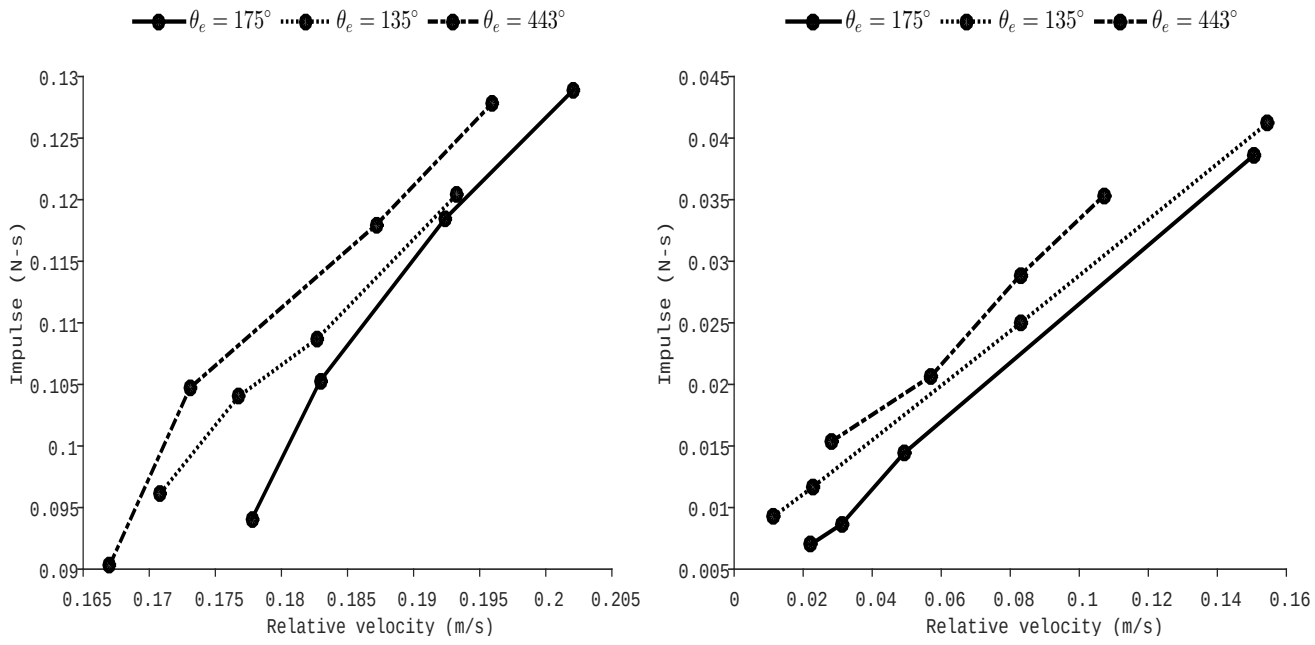

Rotating target Stationary target

Figure 4.20. : Impulse in closed-loop systems

From Fig. 4.20, it has been observed that the magnitude of the impulse is varying linearly with respect to relative velocity as in open-loop impact. The different angles of approach have

different values for impulse. Also the impulse is high for rotating objects in comparison to a stationary object.

All the results and discussion presented in this thesis would be very helpful for designing and modeling a multi-arm space robot for capturing operations. The post impact dynamics would help in studying the behaviour of the system in the post impact phase. This could be validated with experimental results. The investigations done to study the variation of impulsive forces with relative velocity and angle of approach can be very helpful for designing any post impact control strategy. Such kind of strategy is essential because uncontrolled dynamics would result in undesirable motion. The above results also validated the framework presented to model impact dynamics.

...

5
Conclusion and Future work

In conclusion, it may be said that this research work has given rise to a framework for pre-impact, impact and post-impact modeling for multi-arm space robot. First the kinematic and dynamic equations of multi-arm robot and target object has been formulated, which are then used in impact modeling. The impact of two or more orbiting targets with multiple arms of a space robot have been modeled as open-loop impact and the impact of one target with multiple arms have been modeled as closed-loop impact. The post impact dynamics has been simulated for the multi-arm robot while capturing orbiting object.

This research work has also used MATLAB based general purpose software named Recursive Dynamics Simulator (ReDySim), which essentially consisting of recursive order (n) inverse and forward dynamics algorithms for simulation and control of tree-type fixed- or floating-base robotic system. As the "ReDySim" is generic software for simulating multi-degrees-of-freedom robotic systems, its capability is enhanced for open- and closed-loop impact modeling of floating base systems.

The post impact dynamic simulation results were validated by subjecting robot to impact under different conditions of the target object. Further the laws of inelastic impact are verified by studying momentum of the system, which is remaining conserved before and after impact. The impulse is also investigated during impact along with the effect of relative velocity and angles of approach on it, which would be very useful for designing a control strategy in post-impact phase.

Salient contributions, as a result of this research work are listed below:

1. Kinematic and dynamic modeling of pre-impact, impact and post-impact phases for a multi-

arm floating base robotics system while capturing tumbling orbiting objects.

2. Enhancement of "ReDySim - generic software for simulating multi-degrees-of-freedom robotic systems" capability for open- and closed-loop impact modeling of floating base systems.

3. Numerical experiments of pre-impact, impact and post-impact phases for multi-arm open- and closed-loop impacts and investigating the effects of relative velocity and angle of approach on impact forces.

5.1 FUTURE WORK

This research work has given rise to some useful directions which forms the future scope of research. They are as follows:

1. It may be noted that post impact uncontrolled dynamics will result in undesirable motion, thus a control scheme will be proposed to achieve post-impact stabilization in future work.

2. Experimental implementation and validation of the proposed method on an earth-based dual-arm robot will also be carried out in future.

3. Robots used in space are light in weight. Thus, it is important to introduce flexibility of links as flexible manipulators have the advantage of being light and soft. Softness of robots improves safety at the moment of contact with the object. In future, capturing of an orbiting target object using two flexible manipulators will be modeled and simulated.

...

Appendix A

Kinematic Equations of Dual-arm space robot

For the completeness of the framework proposed in this thesis, the kinematics equations of dual-arm space robot as shown in Fig. 2.3, are given in this appendix. The problem of kinematics is to describe the motion of the manipulator without consideration of the forces and torques causing the motion. First the position kinematics is given, which is to determine the position and orientation of the end-effector given the values for the joint variables of the robot. Second, the velocity kinematics is formulated, which is to determine the velocity of the end-effector given the values for the joint velocities of the robot

A.1 POSITION KINEMATICS

The position (x_i, y_i) and orientation (θ_i) of end-effector 1 and 2 for dual-arm space robot as shown in Fig. 2.3 can be written as

$$x_{e1} = x_0 + \frac{a_0}{2}c_0 + a_1 c_{01} + a_2 c_{012}$$

$$y_{e1} = y_0 + \frac{a_0}{2}s_0 + a_1 s_{01} + a_2 s_{012}$$

$$\theta_{e1} = \theta_0 + \theta_1 + \theta_2$$

$$x_{e2} = x_0 + \frac{a_0}{2}c_0 + a_3 c_{03}$$

$$y_{e2} = y_0 + \frac{a_0}{2}s_0 + a_3 s_{03}$$

$$\theta_{e2} = \theta_0 + \theta_3 \tag{A.1}$$

A.2 VELOCITY KINEMATICS

The end-effector's velocity can be obtained by differentiating equation (A.1) w.r.t time as

$$\dot{x_{e1}} = \dot{x_0} - \frac{a_0}{2} s_0 \dot{\theta_0} - a_1 s_{01} \dot{\theta_{01}} - a_2 s_{012} \dot{\theta_{012}}$$

$$\dot{y_{e1}} = \dot{y_0} + \frac{a_0}{2} c_0 \dot{\theta_0} + a_1 c_{01} \dot{\theta_{01}} + a_2 c_{012} \dot{\theta_{012}}$$

$$\dot{\theta_{e1}} = \dot{\theta_0} + \dot{\theta_1} + \dot{\theta_2}$$

$$\dot{x_{e2}} = \dot{x_0} - \frac{a_0}{2} s_0 \dot{\theta_0} - a_3 s_{03} \dot{\theta_{03}}$$

$$\dot{y_{e2}} = \dot{y_0} + \frac{a_0}{2} c_0 \dot{\theta_0} + a_3 c_{03} \dot{\theta_{03}}$$

$$\dot{\theta_{e2}} = \dot{\theta_0} + \dot{\theta_3} \tag{A.2}$$

The end-effector's velocities are expressed in terms of the base velocity (t_b) and joint velocity ($\dot{\theta}$) as

$$\begin{bmatrix} t_{e1} \\ t_{e2} \end{bmatrix} = \begin{bmatrix} J_{b1} \\ J_{b2} \end{bmatrix} t_b + \begin{bmatrix} J_{m1} & O \\ O & J_{m2} \end{bmatrix} \dot{\theta} \tag{A.3}$$

where t_{e1} and t_{e2} is twists of end-effector 1 and 2, respectively. J_{b1} and J_{b2} is the jacobian matrices from base to end-effector 1 and 2, respectively. J_{m1} and J_{m2} is the jacobian matrices for manipulator 1 and 2, respectively. O is the null matrix of compatible dimension. For the system under study they are written as

$$t_{e1} = \begin{bmatrix} \dot{x}_{e1} & \dot{y}_{e1} & \dot{\theta}_{e1} \end{bmatrix}^T, \; t_{e2} = \begin{bmatrix} \dot{x}_{e2} & \dot{y}_{e2} & \dot{\theta}_{e2} \end{bmatrix}^T$$

$$J_{b1} = \begin{bmatrix} 1 & 0 & -\frac{a_0}{2} s_0 - a_1 s_{01} - a_2 s_{012} \\ 0 & 1 & \frac{a_0}{2} c_0 + a_1 c_{01} + a_2 c_{012} \\ 0 & 0 & 1 \end{bmatrix}, \; J_{b2} = \begin{bmatrix} 1 & 0 & -\frac{a_0}{2} s_0 - a_3 s_{03} \\ 0 & 1 & \frac{a_0}{2} c_0 + a_3 c_{03} \\ 0 & 0 & 1 \end{bmatrix}$$

$$J_{m1} = \begin{bmatrix} -a_1 s_{01} - a_2 s_{012} & -a_2 s_{012} \\ a_1 c_{01} + a_2 c_{012} & a_2 c_{012} \\ 1 & 1 \end{bmatrix}, \; J_{m2} = \begin{bmatrix} -a_3 s_{03} \\ a_3 c_{03} \\ 1 \end{bmatrix}$$

$$t_b = \begin{bmatrix} \dot{x}_0 & \dot{y}_0 & \dot{\theta}_0 \end{bmatrix}^T, \; \dot{\theta} = \begin{bmatrix} \dot{\theta}_1 & \dot{\theta}_2 & \dot{\theta}_3 \end{bmatrix}^T$$

The end-effectors' velocities t_{ei} in (A.3) can also be represented in terms of also joint velocities $\dot{\theta}_i$ using the GJM, as follows

$$\begin{bmatrix} t_{e1} \\ t_{e2} \end{bmatrix} = \begin{bmatrix} J_{g,11} & J_{g,12} \\ J_{g,21} & J_{g,22} \end{bmatrix} \begin{bmatrix} \dot{\theta}_1 \\ \dot{\theta}_2 \\ \dot{\theta}_3 \end{bmatrix} \tag{A.4}$$

where

$J_{g,11} = (J_{m1} - J_{b1} I_b^{-1} I_{bm1}),\ J_{g,12} = (-J_{b1} I_b^{-1} I_{bm2})$

$J_{g,21} = (-J_{b2} I_b^{-1} I_{bm1}),\ J_{g,22} = (J_{m2} - J_{b2} I_b^{-1} I_{bm2}),$

The inertia matrices I_b , I_{bm1} and I_{bm2} have been derived for the same system in Appendix B.

Appendix B

Dynamical Equations of Dual-arm space robot

Dynamic modeling means deriving equations that explicitly describe the relationship between force and motion in a system. To be able to control a robot manipulator as required by its operation, it is important to consider the dynamic model in the design of the control algorithm and simulation of motion. In this appendix, the equations of motions of a space robot are derived using DeNOC approach. Also they are presented in the matrix form to have a better understanding of the general form of EOM for multi-arm space robot. The mathematical model for the dynamic behaviour of the dual-arm planar space robot is developed. A simple model of a space robot, having two arms as shown in Fig. 2.3, is taken for deriving dynamic equations. The following assumptions are made:

1. The mass of the spacecraft is assumed to very high when compared with the mass of the links.
2. Robot arms are not affected by the friction and disturbance.
3. Gravitational force is zero.
4. There are no mechanical restriction nor external forces and torques, so that momentum conservation and equilibrium of forces and moments, strictly hold true during the operation.

B.1 EQUATIONS OF MOTION USING DENOC

The derivation of equations of motion using Decoupled Natural Orthogonal Complement (DeNOC) approach has been taken from Shah et al. (2012a). The vectors of generalized twist and

the generalized independent joint-rates for the $n-$coupled links of a serial module are defined as

$$t = \begin{bmatrix} t_1 & ... & t_i & ... & t_n \end{bmatrix}^T, \; and \; \dot{\theta} = \begin{bmatrix} \dot{\theta}_1 & ... & \dot{\theta}_i & ... & \dot{\theta}_n, \end{bmatrix}^T \tag{B.1}$$

Next, the expression for the generalized twist of a serial module, t, is obtained as

$$t = N\dot{\theta}, \; where \; N = N_l N_d \tag{B.2}$$

The matrices N_l and N_d are referred here as the DeNOC matrices of the serial-module of a tree-type system, which are nothing but those reported by Saha (1997) for a serial robot.

The DeNOC-based methodology for dynamic modeling of a general multibody system, be it serial, tree-type or closed-loop, begins with the uncoupled Newton-Euler (NE) equations of motion of all the links constituting the system. The unconstrained or uncoupled NE equations of motion for the i^{th} rigid-link can be written as (Saha, 1999)

$$I_i^c \dot{\omega}_i + \omega_i \times I_i^c \omega_i = n_i^c$$

$$m_i \dot{v}_i = f_i^c \tag{B.3}$$

For $n-$bodies, $6n-$uncoupled equations of motion are then written in terms of the twist t, twist-rate $\dot{t}$ and wrench w (Saha et al., 2013) as

$$M\dot{t} + \Omega M t = w, \; where \; w = w^E + w^C + w^D \tag{B.4}$$

where

$M = diag\begin{bmatrix} M_1 & ... & M_i & ... & M_n \end{bmatrix}$ and $\Omega = diag\begin{bmatrix} \Omega_1 & ... & \Omega_i & ... & \Omega_n \end{bmatrix}$ are $6n \times 6n$ generalized matrices of mass and angular velocities, respectively,

$w = \begin{bmatrix} w_1^T & ... & w_i^T & ... & w_n^T \end{bmatrix}$ and $t = \begin{bmatrix} t_1^T & ... & t_i^T & ... & t_n^T \end{bmatrix}$ are $6n-$dimensional generalized vectors of wrenches and twists, respectively,

w^E, w^C and w^D are $6n-$dimensional generalized wrenches due to external, constraint and driving moments and forces, respectively.

The matrices M_i, Ω_i, w_i and t_i can be written as

$$M_i = \begin{bmatrix} I_i^c & O \\ O & m_i 1 \end{bmatrix},\ \Omega_i = \begin{bmatrix} \omega_i \times 1 & O \\ O & O \end{bmatrix},\ w_i = \begin{bmatrix} n_i^c \\ f_i^c \end{bmatrix},\ t_i = \begin{bmatrix} \omega_i \\ v_i \end{bmatrix} \tag{B.5}$$

One may show that the pre-multiplication of (B.4) by $N_l^T N_d^T$ yields the minimal set of equations of motion eliminating the constraint wrenches. More specifically, $N_l^T N_d^T w^c = 0$ (Angeles and Lee, 1988). Thus (B.4) leads to

$$N_l^T N_d^T (M\dot{t} + \Omega M t) = N_l^T N_d^T (w^D + w^E) \tag{B.6}$$

Now, substitution of $t = N_l N_d \dot{\theta}$, from (B.2), and its time derivative into (B.6) yields the following equations of motion:

$$I\ddot{\theta} + C\dot{\theta} = \tau + \tau^E \tag{B.7}$$

where the expressions of the Generalized Inertia Matrix (GIM) I, matrix of convective inertia (MCI) terms C, and the vectors of the generalized driving forces τ and the external forces τ^E are given as

$$I = N^T M N,\ C = N^T (MN + \Omega MN),\ \tau = N^T w^D,\ \tau^E = N^T w^E \tag{B.8}$$

(B.8) represents the constrained dynamic equations of motion for a tree-type robotic system with general kinematic module architecture.

Since no external force is acting, so the vector of generalized driving forces for the dual-arm robot shown in 2.3 is given by $\tau = \begin{bmatrix} f_x & f_y & \tau_0 & \tau_1 & \tau_2 \end{bmatrix}^T$. The expression for base forces f_x, f_y and τ_0 and manipulator torques τ_1, τ_2 and τ_3 obained using DeNOC approach are given as

$$f_x = m_0\ddot{x}_0 + m_1\ddot{x}_0 + m_2\ddot{x}_0 + m_3\ddot{x}_0 - m_2 d_{2x}\ddot{\theta}_0 c_{012} - m_2 d_{2x}\dot{\theta}_1^{\,2} c_{012} - m_2 d_{2x}\dot{\theta}_2^{\,2} c_{012} - m_2 a_1 \ddot{\theta}_0 s_{01} - m_2 a_1 \ddot{\theta}_1 s_{01} - m_1 d_{1x}\ddot{\theta}_0 s_{01} - m_1 d_{1x}\ddot{\theta}_1 s_{01} - \tfrac{1}{2}(m_1 a_0 \ddot{\theta}_0 s_0) - \tfrac{1}{2}(m_2 a_0 \ddot{\theta}_0 s_0) - m_2 a_1 \dot{\theta}_0^{\,2} c_{01} - m_2 a_1 \dot{\theta}_1^{\,2} c_{01} - m_1 d_{1x}\dot{\theta}_0^{\,2} c_{01} - m_1 d_{1x}\dot{\theta}_1^{\,2} c_{01} - m_2 d_{2x}\ddot{\theta}_0 s_{012} - m_2 d_{2x}\ddot{\theta}_1 s_{012} - m_2 d_{2x}\ddot{\theta}_2 s_{012} - \tfrac{1}{2}(m_1 a_0 \dot{\theta}_0^{\,2} c_0) - \tfrac{1}{2}(m_2 a_0 \dot{\theta}_0^{\,2} c_0) - 2m_2 d_{2x}\dot{\theta}_0\dot{\theta}_1 c_{012} - 2m_2 d_{2x}\dot{\theta}_0\dot{\theta}_2 c_{012} - 2m_2 d_{2x}\dot{\theta}_1\dot{\theta}_2 c_{012} - 2m_2 a_1 \dot{\theta}_0\dot{\theta}_1 c_{01} - 2m_1 d_{1x}\dot{\theta}_0\dot{\theta}_1 c_{01} + \tfrac{1}{2}(a_0 m_3 s_0 \ddot{\theta}_0) + d_{3x} m_3 s_{03}\ddot{\theta}_{03} + d_{3x} m_3 s_{03}\ddot{\theta}_3 + d_{3x}\dot{\theta}_0^{\,2} m_3 c_{03} + d_{3x}\dot{\theta}_3^{\,2} m_3 c_{03} + \tfrac{1}{2} a_0 \dot{\theta}_0^{\,2} m_3 c_0 + 2d_{3x}\dot{\theta}_0\dot{\theta}_3 m_3 c_{03}$$

$$f_y = m_0\ddot{y}_0 + m_1\ddot{y}_0 + m_2\ddot{y}_0 + m_3\ddot{y}_0 - m_2 d_{2x}\ddot{\theta}_0 s_{012} - m_2 d_{2x}\dot{\theta}_1^{\,2} s_{012} - m_2 d_{2x}\dot{\theta}_2^{\,2} s_{012} + m_2 a_1 \ddot{\theta}_0 c_{01} + m_2 a_1 \ddot{\theta}_1 c_{01} + m_1 d_{1x}\ddot{\theta}_0 c_{01} + m_1 d_{1x}\ddot{\theta}_1 c_{01} + \tfrac{1}{2}(m_1 a_0 \ddot{\theta}_0 c_0) + \tfrac{1}{2}(m_2 a_0 \ddot{\theta}_0 c_0) - m_2 a_1 \dot{\theta}_0^{\,2} s_{01} - m_2 a_1 \dot{\theta}_1^{\,2} s_{01} - m_1 d_{1x}\dot{\theta}_0^{\,2} s_{01} - m_1 d_{1x}\dot{\theta}_1^{\,2} s_{01} + m_2 d_{2x}\ddot{\theta}_0 c_{012} + m_2 d_{2x}\ddot{\theta}_1 c_{012} + m_2 d_{2x}\ddot{\theta}_2 c_{012} - \tfrac{1}{2}(m_1 a_0 \dot{\theta}_0^{\,2} s_0) - \tfrac{1}{2}(m_2 a_0 \dot{\theta}_0^{\,2} s_0) - 2m_2 d_{2x}\dot{\theta}_0\dot{\theta}_1 s_{012} - 2m_2 d_{2x}\dot{\theta}_0\dot{\theta}_2 s_{012} - 2m_2 d_{2x}\dot{\theta}_1\dot{\theta}_2 s_{012} - 2m_2 a_1 \dot{\theta}_0\dot{\theta}_1 s_{01} - 2m_1 d_{1x}\dot{\theta}_0\dot{\theta}_1 s_{01} - \tfrac{1}{2}(a_0 m_3 c_0 \ddot{\theta}_0) - d_{3x} m_3 c_{03}\ddot{\theta} - d_{3x} m_3 c_{03}\ddot{\theta}_3 + d_{3x}\dot{\theta}_0^{\,2} m_3 s_{03} + d_{3x}\dot{\theta}_3^{\,2} m_3 s_{03} + \tfrac{1}{2}(a_0\dot{\theta}_0^{\,2} m_3 s_0) + 2d_{3x}\dot{\theta}_0\dot{\theta}_3 m_3 s_{03}$$

$$\tau_0 = I_{0z}\ddot{\theta}_0 + I_{1z}\ddot{\theta}_0 + I_{2z}\ddot{\theta}_0 + I_{1z}\ddot{\theta}_1 + I_{2z}\ddot{\theta}_1 + I_{2z}\ddot{\theta}_2 + \tfrac{1}{4}(m_1 a_0^2\ddot{\theta}_0) + \tfrac{1}{4}(m_2 a_0^2\ddot{\theta}_0) + m_2 a_1^2\ddot{\theta}_0 + m_2 a_1^2\ddot{\theta}_1 + m_1 d_{1x}^2\ddot{\theta}_0 + m_2 d_{2x}^2\ddot{\theta}_0 + m_1 d_{1x}^2\ddot{\theta}_1 + m_2 d_{2x}^2\ddot{\theta}_1 + m_2 d_{2x}^2\ddot{\theta}_2 + m_2 a_1\ddot{y}_0 c_{01} - m_1 a_0\ddot{x}_0 s_0 - \tfrac{1}{2}(m_2 a_0\ddot{x}_0 s_0) + m_1 d_{1x}\ddot{y}_0 c_{01} - m_2 a_1\ddot{x}_0 s_{01} - m_1 d_{1x}\ddot{x}_0 s_{01} + \tfrac{1}{2}(m_1 a_0\ddot{y}_0 c_0) + \tfrac{1}{2}(m_2 a_0\ddot{y}_0 c_0) + m_2 d_{2x}\ddot{y}_0 c_{012} - m_2 d_{2x}\ddot{x}_0 s_{012} - \tfrac{1}{2}(m_2 a_0 d_{2x}\dot{\theta}_1^{\,2} s_{12}) - \tfrac{1}{2}(m_2 a_0 d_{2x}\dot{\theta}_2^{\,2} s_{12}) - m_2 a_1 d_{2x}\dot{\theta}_2^{\,2} s_2 - \tfrac{1}{2}(m_1 a_0 d_{1x}\dot{\theta}_1^{\,2} s_1) + m_2 a_0 d_{2x}\ddot{\theta}_0 c_{12} + \tfrac{1}{2}(m_2 a_0 d_{2x}\ddot{\theta}_1 c_{12}) + \tfrac{1}{2}(m_2 a_0 d_{2x}\ddot{\theta}_2 c_{12}) + m_2 a_0 a_1\ddot{\theta}_0 c_1 + 2m_2 a_1 d_{2x}\ddot{\theta}_0 c_2 + \tfrac{1}{2}(m_1 a_0 d_{1x}\ddot{\theta}_1 c_1) + 2m_2 a_1 d_{2x}\ddot{\theta}_1 c_2 + m_2 a_1 d_{2x}\ddot{\theta}_2 c_2 - m_2 a_0 d_{2x}\dot{\theta}_0\dot{\theta}_1 s_{12} - m_2 a_0 d_{2x}\dot{\theta}_0\dot{\theta}_2 s_{12} - m_2 a_0 d_{2x}\dot{\theta}_1\dot{\theta}_2 s_{12} - m_2 a_0 a_1\dot{\theta}_0 s_1 - m_1 a_0 d_{1x}\dot{\theta}_0\dot{\theta}_1 s_1 - 2m_2 a_1 d_{2x}\dot{\theta}_0\dot{\theta}_2 s_1 - 2m_2 a_1 d_{2x}\dot{\theta}_1\dot{\theta}_2 s_2 + \tfrac{1}{2}(a_0 m_3 s_0\ddot{x}_0) + d_{3x} m_3 s_{03}\ddot{x}_0 - \tfrac{1}{2}(a_0 m_3 c_0\ddot{y}_0) + d_{3x} m_3 c_{03}\ddot{y}_0 + I_{3z}\ddot{\theta}_0 + d_{3x}^2 m_3\ddot{\theta}_0 + a_0 d_{3x} m_3 c_3\ddot{\theta}_0 + m_3 d_{3x}^2\ddot{\theta}_3 + \tfrac{1}{2}(a_0 m_3 c_3 d_{3x}\ddot{\theta}_3) + I_{3z}\ddot{\theta}_3 + \tfrac{1}{2}(a_0 m_1\dot{x}_0\dot{\theta}_0 c_0) + d_{1x} m_1\dot{x}_0\dot{\theta}_0 c_{01} + d_{1x} m_1\dot{x}_0\dot{\theta}_1 c_{01} + \tfrac{1}{2}(a_0 m_1\dot{y}_0\dot{\theta}_0 s_0) + d_{1x} m_1\dot{y}_0\dot{\theta}_0 s_{01} + d_{1x} m_1\dot{y}_0\dot{\theta}_1 s_{01} + (a_0 m_2\dot{x}_0\dot{\theta}_0 c_0)/2 + a_1 m_2\dot{x}_0\dot{\theta}_0 c_{01} + a_1 m_2\dot{x}_0\dot{\theta}_1 c_{01} + d_{2x} m_2\dot{x}_0\dot{\theta}_0 c_{013} + d_{2x} m_2\dot{x}_0\dot{\theta}_1 c_{013} + d_{2x} m_2\dot{x}_0\dot{\theta}_2 c_{013} + \tfrac{1}{2}(a_0 m_2\dot{y}_0\dot{\theta}_0 s_0) + a_1 m_2\dot{y}_0\dot{\theta}_0 s_{01} + a_1 m_2\dot{y}_0\dot{\theta}_1 s_{01} + d_{2x} m_2\dot{y}_0\dot{\theta}_0 s_{013} + d_{2x} m_2\dot{y}_0\dot{\theta}_1 s_{013} + d_{2x} m_2\dot{y}_0\dot{\theta}_2 s_{013}) - \tfrac{1}{2}(a_0 d_{3x}\dot{\theta}_3^{\,2} m_3 s_3) + a_0 d_{3x}\dot{\theta}_0\dot{\theta}_3 m_3 s_3 - \tfrac{1}{2}(a_0 m_3\dot{x}_0\dot{\theta}_0 c_0) - d_{3x} m_3\dot{x}_0\dot{\theta}_0 c_{03} - d_{3x} m_3\dot{x}_0\dot{\theta}_3 c_{03} - \tfrac{1}{2}(a_0 m_3\dot{y}_0\dot{\theta}_0 c_0) - d_{3x} m_3\dot{y}_0\dot{\theta}_0 s_{03} - d_{3x} m_3\dot{y}_0\dot{\theta}_3 s_{03}$$

$$\tau_1 = I_{1z}\ddot{\theta}_0 + I_{2z}\ddot{\theta}_0 + I_{1z}\ddot{\theta}_1 + I_{2z}\ddot{\theta}_1 + I_{2z}\ddot{\theta}_2 + m_2 a_1^2\ddot{\theta}_0 + m_2 a_1^2\ddot{\theta}_1 + m_1 d_{1x}^2\ddot{\theta}_0 + m_2 d_{2x}^2\ddot{\theta}_0 + m_1 d_{1x}^2\ddot{\theta}_1 + m_2 d_{2x}^2\ddot{\theta}_2 + m_2 a_1\ddot{y}_0 c_{01} + m_1 d_{1x}\ddot{y}_0 c_{01} - m_2 a_1\ddot{x}_0 s_{01} - m_2 d_{1x}\ddot{x}_0 s_{01} + m_2 d_{2x}\ddot{y}_0 c_{012} - m_2 d_{2x}\ddot{x}_0 s_{012} + \tfrac{1}{2}(m_2 a_0 d_{2x}\ddot{\theta}_0 c_{12}) + \tfrac{1}{2}(m_2 a_0 a_1\ddot{\theta}_0 c_1) + \tfrac{1}{2}(m_1 a_0 d_{1x}\ddot{\theta}_0 c_1) + 2m_2 a_1 d_{2x}\ddot{\theta}_0 c_2 + 2m_2 a_1 d_{2x}\ddot{\theta}_1 c_2 + m_2 a_1 d_{2x}\ddot{\theta}_2 c_2 - (\tfrac{1}{2}(a_0 d_{2x}\dot{\theta}_0\dot{\theta}_1 m_2 s_{12}) + \tfrac{1}{2}(a_0 d_{2x}\dot{\theta}_0\dot{\theta}_2 m_2 s_{12}) + \tfrac{1}{2}(a_0 a_1\dot{\theta}_0\dot{\theta}_1 m_2 s_1) - \tfrac{1}{2}(a_0 d_{1x}\dot{\theta}_0\dot{\theta}_1 m_1 s_1) + a_1 d_{2x}\dot{\theta}_2^{\,2} m_2 s_2 + 2a_1 d_{2x}\dot{\theta}_0\dot{\theta}_2 m_2 s_2 + 2a_1 d_{2x}\dot{\theta}_1\dot{\theta}_2 m_2 s_2 + d_{1x} m_1\dot{x}_0\dot{\theta}_0 c_{01} + d_{1x} m_1\dot{x}_0\dot{\theta}_1 c_{01} + d_{1x} m_1\dot{y}_0\dot{\theta}_0 s_{01} + d_{1x} m_1\dot{y}_0\dot{\theta}_1 s_{01} + 2d_{1x} m_2\dot{x}_0\dot{\theta}_0 c_{01} + 2d_{1x} m_2\dot{x}_0\dot{\theta}_1 c_{01} + d_{2x} m_2\dot{x}_0\dot{\theta}_0 c_{012} + d_{2x} m_2\dot{x}_0\dot{\theta}_1 c_{012} + d_{2x} m_2\dot{x}_0\dot{\theta}_2 c_{012} + 2d_{1x} m_2\dot{y}_0\dot{\theta}_0 s_{01} + 2d_{1x} m_2\dot{y}_0\dot{\theta}_1 s_{01} + d_{2x} m_2\dot{y}_0\dot{\theta}_0 s_{012} + d_{2x} m_2\dot{y}_0\dot{\theta}_1 s_{012} + d_{2x} m_2\dot{y}_0\dot{\theta}_2 s_{012})$$

$$\tau_2 = I_{2z}\ddot{\theta}_0 + I_{2z}\ddot{\theta}_1 + I_{2z}\ddot{\theta}_2 + m_2 d_{2x}^2\ddot{\theta}_0 + m_2 d_{2x}^2\ddot{\theta}_1 + m_2 d_{2x}^2\ddot{\theta}_2 + m_2 d_{2x}\ddot{y}_0 c_{012} - m_2 d_{2x}\ddot{x}_0 s_{012} + \tfrac{1}{2}(m_2 a_0 d_{2x}\ddot{\theta}_0 c_{12}) + m_2 a_1 d_{2x}\ddot{\theta}_0 c_2 + m_2 a_1 d_{2x}\ddot{\theta}_1 c_2 - (a_1 d_{2x} m_2 \dot{\theta}_0\dot{\theta}_2 s_2 + a_1 d_{2x} m_2 \dot{\theta}_1\dot{\theta}_2 s_2 + \tfrac{1}{2}(a_0 d_{2x} m_2 \dot{\theta}_0\dot{\theta}_1 s_{12}) + \tfrac{1}{2}(a_0 d_{2x} m_2 \dot{\theta}_0\dot{\theta}_2 s_{12}) + \tfrac{1}{2}(a_0 d_{2x} m_2 \dot{\theta}_1^{\,2} s_{12}) + \tfrac{1}{2}(a_0 d_{2x} m_2 \dot{\theta}_1\dot{\theta}_2 s_{12}) + d_{2x} m_2 \dot{x}_0\dot{\theta}_0 c_{012} + d_{2x} m_2 \dot{x}_0\dot{\theta}_1 c_{012} + d_{2x} m_2 \dot{x}_0\dot{\theta}_2 c_{012} + d_{2x} m_2 \dot{y}_0\dot{\theta}_0 s_{012} + d_{2x} m_2 \dot{y}_0\dot{\theta}_1 s_{012} + d_{2x} m_2 \dot{y}_0\dot{\theta}_2 s_{012}$$

$$\tau_3 = d_{3x} m_3 s_{03}\ddot{x}_0 - d_{3x} m_3 c_{03}\ddot{y}_0 + m_3 d_{3x}^2\ddot{\theta}_0 + \tfrac{1}{2}(a_0 m_3 c_3 d_{3x}\ddot{\theta}_0) + I_{3z}\ddot{\theta}_0 + m_3 d_{3x}^2\ddot{\theta}_3 + I_{3z}\ddot{\theta}_3 + \tfrac{1}{2}(a_0 d_{3x}\dot{\theta}_0^{\,2} m_3 s_3) + d_{3x} m_3 \dot{x}_0\dot{\theta}_0 c_{03} + d_{3x} m_3 \dot{x}_0\dot{\theta}_3 c_{03} + \tfrac{1}{2}(d_{3x} m_3 \dot{y}_0\dot{\theta}_0 s_{03}) + \tfrac{1}{2}(d_{3x} m_3 \dot{y}_0\dot{\theta}_3 s_{03})$$

B.2 MATRIX FORMULATION

The above generalized forces can be re-arranged in matrix form. The equations of motion for a dual-arm space robot shown in Fig. 2.3 can be written in matrix form as

$$\begin{bmatrix} I_b & I_{bm1} & I_{bm2} \\ I_{bm1}^T & I_{m1} & O \\ I_{bm2}^T & O & I_{m2} \end{bmatrix} \begin{bmatrix} \dot{t}_b \\ \ddot{\theta}_{m1} \\ \ddot{\theta}_{m2} \end{bmatrix} + \begin{bmatrix} c_b \\ c_{m1} \\ c_{m2} \end{bmatrix} = \begin{bmatrix} F_b \\ \tau_{m1} \\ \tau_{m2} \end{bmatrix} \tag{B.9}$$

where

$$I_b = \begin{bmatrix} I_{b11} & I_{b12} & I_{b13} \\ I_{b21} & I_{b22} & I_{b23} \\ I_{b31} & I_{b32} & I_{b33} \end{bmatrix},\ I_{bm1} = \begin{bmatrix} I_{bm14} & I_{bm15} \\ I_{bm24} & I_{bm25} \\ I_{bm34} & I_{bm35} \end{bmatrix},\ I_{bm2} = \begin{bmatrix} I_{bm16} \\ I_{bm26} \\ I_{bm36} \end{bmatrix},\ I_{m1} = \begin{bmatrix} I_{m44} & I_{m45} \\ I_{m54} & I_{m55} \end{bmatrix},\ I_{m2} = \begin{bmatrix} I_{m66} \end{bmatrix}$$

$$\dot{t}_b = \begin{bmatrix} \ddot{x}_0 & \ddot{y}_0 & \ddot{\theta}_0 \end{bmatrix}^T,\ \ddot{\theta}_{m1} = \begin{bmatrix} \ddot{\theta}_1 & \ddot{\theta}_2 \end{bmatrix}^T,\ \ddot{\theta}_{m2} = \begin{bmatrix} \ddot{\theta}_3 \end{bmatrix}$$
$$c_b = \begin{bmatrix} c_{b1} & c_{b2} & c_{b3} \end{bmatrix}^T,\ c_{m1} = \begin{bmatrix} c_1 & c_2 \end{bmatrix}^T,\ c_{m2} = \begin{bmatrix} c_3 \end{bmatrix}$$
$$f_b = \begin{bmatrix} f_{bx} & f_{by} & \tau_0 \end{bmatrix}^T,\ \tau_{m1} = \begin{bmatrix} \tau_1 & \tau_2 \end{bmatrix}^T,\ \tau_{m2} = \begin{bmatrix} \tau_3 \end{bmatrix}$$

In the above,

$I_{b11} = m_0 + m_1 + m_2 + m_3$

$I_{b12} = 0$

$$I_{b13} = -m_2 a_1 s_{01} - m_1 d_{1x} s_{01} - m_1 a_0 s_0/2 - m_2 a_0 s_0/2 - m_2 d_{2x} s_{012} + a_0 m_3 s_0/2 + d_{3x} m_3 s_{03}$$

$$I_{bm_1 4} = -m_2 a_1 s_{01} - m_1 d_{1x} \ddot{\theta}_1 s_{01} - m_2 d_{2x} s_{012}$$

$$I_{bm15} = -m_2 d_{2x} s_{012}$$

$$I_{bm16} = d_{3x} m_3 s_{03}$$

$$I_{b21} = 0$$

$$I_{b22} = m_0 + m_1 + m_2 + m_3$$

$$I_{b23} = m_2 a_1 c_{01} + m_1 d_{1x} c_{01} + m_1 a_0 c_0/2 + m_2 a_0 c_0/2 + m_2 d_{2x} c_{012} - a_0 m_3 c_0/2 - d_{3x} m_3 c_{03}$$

$$I_{bm24} = m_2 a_1 c_{01} + m_1 d_{1x} c_{01} + m_2 d_{2x} c_{012}$$

$$I_{bm25} = m_2 d_{2x} c_{012}$$

$$I_{bm26} = -d_{3x} m_3 c_{03}$$

$$I_{b31} = -m_2 a_1 s_{01} - m_1 d_{1x} s_{01} - m_1 a_0 s_0/2 - m_2 a_0 s_0/2 - m_2 d_{2x} s_{012} + a_0 m_3 s_0/2 + d_{3x} m_3 s_{03}$$

$$I_{b32} = m_2 a_1 c_{01} + m_1 d_{1x} c_{01} + m_1 a_0 c_0/2 + m_2 a_0 c_0/2 + m_2 d_{2x} c_{012} - (a_0 m_3 c_0)/2 - d_{3x} m_3 c_{03}$$

$$I_{b33} = (I_{0z} + I_{1z} + I_{2z}) + m_1 a_0^2/4 + m_2 a_0^2/4 + m_2 a_1^2 + m_1 d_{1x}^2 + m_2 d_{2x}^2 + m_2 a_0 d_{2x} c_{12} + m_2 a_0 a_1 c_1 + m_1 a_0 d_{1x} c_1 +$$

$$2 a_1 d_{2x} c_2 + I_{3z} + d_{3x}^2 m_3 + a_0 d_{3x} m_3 c_3$$

$$I_{bm34} = (I_{1z} + I_{2z}) + m_2 a_1^2 + m_1 d_{1x}^2 + m_2 d_{2x}^2 + m_2 a_0 d_{2x} c_{12}/2 + m_2 a_0 a_1 c_1/2 + m_1 a_0 d_{1x} c_1/2 + 2 a_1 d_{2x} c_2$$

$$I_{bm35} = I_{2z} + m_2 d_{2x}^2 + m_2 a_0 d_{2x} c_{12}/2 + m_2 a_1 d_{2x} c_2$$

$$I_{bm36} = m_3 d_{3x}^2 + (a_0 m_3 c_3 d_{3x})/2 + I_{3z}$$

$$I_{m44} = (I_{1z} + I_{2z}) + m_2 a_1^2 + m_1 d_{1x}^2 + m_2 d_{2x}^2 + 2 m_2 a_1 d_{2x} c_2$$

$$I_{m45} = I_{2z} + m_2 d_{2x}^2 + m_2 a_1 d_{2x} c_2$$

$$I_{m54} = I_{2z} + m_2 d_{2x}^2 + m_2 a_1 d_{2x} c_2$$

$$I_{m55} = I_{2z} + m_2 d_{2x}^2$$

$$I_{m66} = m_3 d_{3x}^2 + I_{3z}$$

$$c_{b1} = -m_2 d_{2x} \dot{\theta_0}^2 c_{012} - m_2 a_1 \dot{\theta_0}^2 c_{01} - m_1 d_{1x} \dot{\theta_0}^2 c_{01} - m_1 a_0 \dot{\theta_0}^2 c_0/2 - m_2 a_0 \dot{\theta_0}^2 c_0/2 - 2m_2 d_{2x} \dot{\theta_0} \dot{(\theta_2)} c_{012}$$
$$- m_2 d_{2x} \dot{\theta_1}^2 c_{012} - m_2 a_1 \dot{\theta_1}^2 c_{01} - m_1 d_{1x} \dot{\theta_1}^2 c_{01} - 2m_2 d_{2x} \dot{\theta_0} \dot{\theta_1} c_{012} - 2m_2 a_1 \dot{\theta_0} \dot{\theta_1} c_{01} - 2m_1 d_{1x} \dot{\theta_0} \dot{\theta_1} c_{01}$$
$$- m_2 d_{2x} \dot{\theta_2}^2 c_{012} - 2m_2 d_{2x} \dot{\theta_1} \dot{\theta_2} c_{012} + d_3 x \dot{\theta_0}^2 m_3 c_0 3 + d_{3x} \dot{\theta_3}^2 m_3 c_{03} + (a_0 \dot{\theta_0}^2 m_3 c_0)/2 + 2d_{3x} \dot{\theta_0} \dot{\theta_3} m_3 c_{03}$$

$$c_{b2} = -m_2 d_{2x} \dot{\theta_0}^2 s_{012} - m_2 a_1 \dot{\theta_0}^2 s_{01} - m_1 d_{1x} \dot{\theta_0}^2 s_{01} - m_1 a_0 \dot{\theta_0}^2 s_0/2 - m_2 a_0 \dot{\theta_0}^2 s_0/2 - 2m_2 d_{2x} \dot{\theta_0} \dot{\theta_2} s_{012}$$
$$- m_2 d_{2x} \dot{\theta_1}^2 s_{012} - m_2 a_1 \dot{\theta_1}^2 s_{01} - m_1 d_{1x} \dot{\theta_1}^2 s_{01} - 2m_2 d_{2x} \dot{\theta_0} \dot{\theta_1} s_{012} - 2m_2 a_1 \dot{\theta_0} \dot{\theta_1} s_{01} - 2m_1 d_{1x} \dot{\theta_0} \dot{\theta_1} s_{01}$$
$$- m_2 d_{2x} \dot{\theta_2}^2 s_{012} - 2m_2 d_{2x} \dot{(\theta_1)} \dot{(\theta_2)} s_{012} + d_{3x} \dot{\theta_0}^2 m_3 s_{03} + d_{3x} \dot{\theta_3}^2 m_3 s_0 3 + (a_0 \dot{\theta_0}^2 m_3 s_0)/2 + 2d_{3x} \dot{\theta_0} \dot{\theta_3} m_3 s_{03}$$

$$c_{b3} = -m_2 a_0 d_{2x} \dot{\theta_0} \dot{\theta_2} s_{12} - 2m_2 a_1 d_{2x} \dot{\theta_0} \dot{\theta_2} s_2 - m_2 a_0 d_{2x} \dot{\theta_1}^2 s_{12}/2 - m_2 a_0 a_1 \dot{\theta_1}^2 s_1/2 - m_1 a_0 d_{1x} \dot{\theta_1}^2 s_1/2$$
$$- m_2 a_0 d_{2x} \dot{\theta_0} \dot{\theta_1} s_{12} - m_2 a_0 a_1 \dot{\theta_0} \dot{\theta_1} s_1 - m_1 a_0 d_{1x} \dot{\theta_0} \dot{\theta_1} s_1 - m_2 a_0 d_{2x} \dot{\theta_2}^2 s_{12}/2 - m_2 a_1 d_{2x} \dot{\theta_2}^2 s_2 - m_2 a_0 d_{2x} \dot{\theta_1} \dot{\theta_2} s_{12}$$
$$- 2m_2 a_1 d_{2x} \dot{\theta_1} \dot{\theta_2} s_2 + a_0 m_1 \dot{x_0} \dot{\theta_0} c_0)/2 + d_{1x} m_1 \dot{x_0} \dot{\theta_0} c_{01} + d_{1x} m_1 \dot{x_0} \dot{\theta_1} c_{01} + (a_0 m_1 \dot{y_0} \dot{\theta_0} s_0)/2 + d_{1x} m_1 \dot{y_0} \dot{\theta_0} s_{01}$$
$$+ d_{1x} m_1 \dot{y_0} \dot{\theta_1} s_{01} + (a_0 m_2 \dot{x_0} \dot{\theta_0} c_0)/2 + a_1 m_2 \dot{x_0} \dot{\theta_0} c_{01} + a_1 m_2 \dot{x_0} \dot{\theta_1} c_{01} + d_{2x} m_2 \dot{x_0} \dot{\theta_0} c_{013} + d_{2x} m_2 \dot{x_0} \dot{\theta_1} c_{013}$$
$$+ d_{2x} m_2 \dot{x_0} \dot{\theta_2} c_{013} + (a_0 m_2 \dot{y_0} \dot{\theta_0} s_0)/2 + a_1 m_2 \dot{y_0} \dot{\theta_0} s_{01} + a_1 m_2 \dot{y_0} \dot{\theta_1} s_{01} + d_{2x} m_2 \dot{y_0} \dot{\theta_0} s_{013} + d_{2x} m_2 \dot{y_0} \dot{\theta_1} s_{013}$$
$$+ d_{2x} m_2 \dot{y_0} \dot{\theta_2} s_{013} - (a_0 d_{3x} \dot{\theta_3}^2 m_3 s_3)/2 + a_0 d_{3x} \dot{\theta_0} \dot{\theta_3} m_3 s_3 - (a_0 m_3 \dot{x_0} \dot{\theta_0} c_0)/2 - d_{3x} m_3 \dot{x_0} \dot{\theta_0} c_{03}$$
$$- d_{3x} m_3 \dot{x_0} \dot{\theta_3} c_{03} - (a_0 m_3 \dot{y_0} \dot{\theta_0} c_0)/2 - d_{3x} m_3 \dot{y_0} \dot{\theta_0} s_{03} - d_{3x} m_3 \dot{y_0} \dot{\theta_3} s_{03}$$

$$c_1 = -((a_0 d_{2x} \dot{\theta_0} \dot{\theta_1} m_2 s_{12})/2 + (a_0 d_{2x} \dot{\theta_0} \dot{\theta_2} m_2 s_{12})/2 + (a_0 a_1 \dot{\theta_0} \dot{\theta_1} m_2 s_1)/2 - (a_0 d_{1x} \dot{\theta_0} \dot{\theta_1} m_1 s_1)/2$$
$$+ a_1 d_{2x} \dot{\theta_2}^2 m_2 s_2 + 2a_1 d_{2x} \dot{\theta_0} \dot{\theta_2} m_2 s_2 + 2a_1 d_{2x} \dot{\theta_1} \dot{\theta_2} m_2 s_2 + d_{1x} m_1 \dot{x_0} \dot{\theta_0} c_{01} + d_{1x} m_1 \dot{x_0} \dot{\theta_1} c_{01} + d_{1x} m_1 \dot{y_0} \dot{\theta_0} s_{01}$$
$$+ d_{1x} m_1 \dot{y_0} \dot{\theta_1} s_{01} + 2d_{1x} m_2 \dot{x_0} \dot{\theta_0} c_{01} + 2d_{1x} m_2 \dot{x_0} \dot{\theta_1} c_{01} + d_{2x} m_2 \dot{x_0} \dot{\theta_0} c_{013} + d_{2x} m_2 \dot{x_0} \dot{\theta_1} c_{013} + d_{2x} m_2 \dot{x_0} \dot{\theta_2} c_{013}$$
$$+ 2d_{1x} m_2 \dot{y_0} \dot{\theta_0} s_{01} + 2d_{1x} m_2 \dot{y_0} \dot{\theta_1} s_{01} + d_{2x} m_2 \dot{y_0} \dot{\theta_0} s_{013} + d_{2x} m_2 \dot{y_0} \dot{\theta_1} s_{013} + d_{2x} m_2 \dot{y_0} \dot{\theta_2} s_{013})$$

$$c_2 = -(a_1 d_{2x} m_2 \dot{\theta}_0 \dot{\theta}_2 s_2 + a_1 d_{2x} m_2 \dot{\theta}_1 \dot{\theta}_2 s_2 + (a_0 d_{2x} m_2 \dot{\theta}_0 \dot{\theta}_1 s_{12})/2 + (a_0 d_{2x} m_2 \dot{\theta}_0 \dot{\theta}_2 s_{12})/2 + (a_0 d_{2x} m_2 \dot{\theta}_1{}^2 s_{12})/2$$

$$+ (a_0 d_{2x} m_2 \dot{\theta}_1 \dot{\theta}_2 s_{12})/2 + d_{2x} m_2 \dot{x_0} \dot{\theta}_0 c_{013} + d_{2x} m_2 \dot{x_0} \dot{\theta}_1 c_{013} + d_{2x} m_2 \dot{x_0} \dot{\theta}_2 c_{013} + d_{2x} m_2 \dot{y_0} \dot{\theta}_0 s_{013}$$

$$+ d_{2x} m_2 \dot{y_0} \dot{\theta}_1 s_{013} + d_{2x} m_2 \dot{y_0} \dot{\theta}_2 s_{013})$$

$$c_3 = (a_0 d_{3x} \dot{\theta}_0{}^2 m_3 s_3)/2 + (d_{3x} m_3 \dot{x_0} \dot{\theta}_0 c_{03} + d_{3x} m_3 \dot{x_0} \dot{\theta}_3 c_{03} + (d_{3x} m_3 \dot{y_0} \dot{\theta}_0 s_{03})/2 + (d_{3x} m_3 \dot{y_0} \dot{\theta}_3 s_{03})/2)$$

Note that in the above expressions, following notations have been used,

$\theta_{01} = \theta_0 + \theta_1,\ \theta_{012} = \theta_0 + \theta_1 + \theta_2,\ \theta_{03} = \theta_0 + \theta_3$

$s_0 = \sin\theta_0,\ s_{01} = \sin(\theta_0 + \theta_1),\ \ s_{012} = \sin(\theta_0 + \theta_1 + \theta_2),\ s_{03} = \sin(\theta_0 + \theta_3)$

$c_0 = \cos\theta_0,\ \ c_{01} = \cos(\theta_0 + \theta_1),\ \ c_{012} = \cos(\theta_0 + \theta_1 + \theta_2),\ c_{03} = \cos(\theta_0 + \theta_3)$

$d_{1x} = \frac{a_1}{2},\ d_{2x} = \frac{a_2}{2},\ d_{3x} = \frac{a_3}{2}$

Appendix C

Momentum Conservation Equations

In this appendix, general form of the momentum conservation equation for a dual-arm space robot, as shown in Fig. 2.3, is derived. This equation serves as a fundamental tool for the control of space manipulators and is extensively used in the thesis. These equations are used to validate the momentum conservation principle during inelastic collision. It also gives a direct relation between the manipulator and base motions which has been used to find base velocities after calculating joint velocities in post-impact phase.

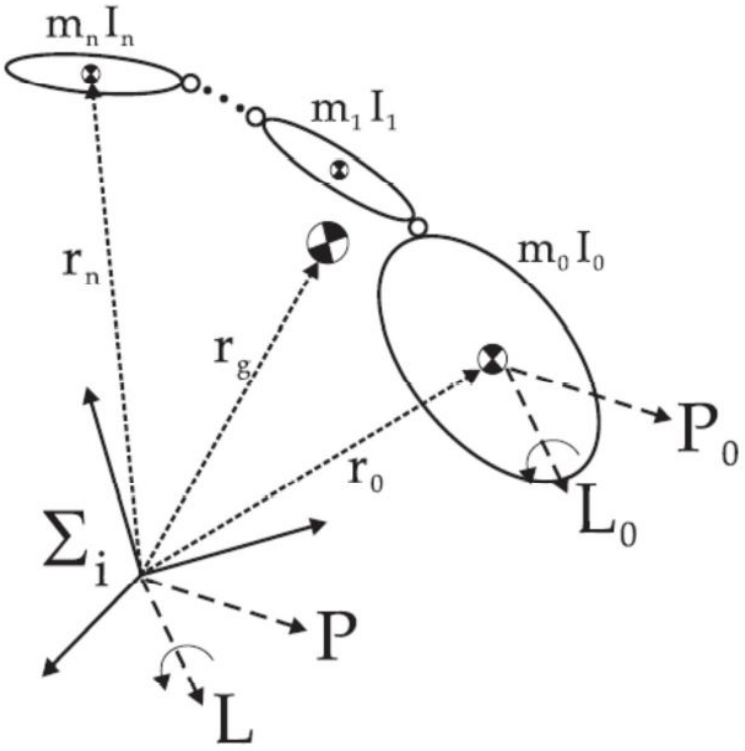

Figure C.1. : A robotic system mounted on a floating or mobile base (Dimitrov, 2006)

C.1 LINEAR MOMENTUM

Linear momentum (p) of the system under study are defined as

$$p = \sum_{i=0}^{n} m_i v_i \tag{C.1}$$

Alternatively, the linear momentum can be expressed using the expression given in (Dimitrov, 2006)

as

$$p = \left(\sum_{i=0}^{n} m_i\right) v_0 + \omega_0 \times \left(\sum_{i=0}^{n} m_i r_i\right) - \left(\sum_{i=0}^{n} m_i\right) \omega_0 \times r_0 + \left(\sum_{i=0}^{n} m_i J_{Ti}\right) \dot{\theta} \tag{C.2}$$

where

$$\sum_{i=0}^{n} m_i = m_0 + m_1 + m_2 + m_3,\ v_0 = \begin{bmatrix} \dot{x}_0 & \dot{y}_0 & 0 \end{bmatrix}^T,\ \omega_0 = \begin{bmatrix} 0 & 0 & \dot{\theta}_0 \end{bmatrix}^T,\ \dot{\theta} = \begin{bmatrix} \dot{\theta}_1 & \dot{\theta}_2 & \dot{\theta}_3 \end{bmatrix}^T$$

$$\sum_{i=0}^{n} m_i r_i = m_0 r_0 + m_1 r_1 + m_2 r_2 + m_3 r_3, \sum_{i=0}^{n} m_i J_{Ti} = m_0 J_{T0} + m_1 J_{T1} + m_2 J_{T2} + m_3 J_{T3}$$

In the above,

$$r_0 = \begin{bmatrix} 0 \\ 0 \\ 0 \end{bmatrix},\ r_1 = \begin{bmatrix} \frac{a_0}{2} c_0 + \frac{a_1}{2} c_{01} \\ \frac{a_0}{2} s_0 + \frac{a_1}{2} s_{01} \\ 0 \end{bmatrix},\ r_2 = \begin{bmatrix} \frac{a_0}{2} c_0 + \frac{a_1}{2} c_{01} + \frac{a_2}{2} c_{012} \\ \frac{a_0}{2} s_0 + \frac{a_1}{2} s_{01} + \frac{a_2}{2} s_{012} \\ 0 \end{bmatrix},\ r_3 = \begin{bmatrix} \frac{a_0}{2} c_0 + \frac{a_3}{2} c_{03} \\ \frac{a_0}{2} s_0 + \frac{a_3}{2} s_{03} \\ 0 \end{bmatrix}$$

$$J_{T0} = \begin{bmatrix} 0 & 0 \\ 0 & 0 \\ 0 & 0 \end{bmatrix},\ J_{T1} = \begin{bmatrix} -\frac{a_1}{2} s_{01} & 0 \\ \frac{a_1}{2} c_{01} & 0 \\ 0 & 0 \end{bmatrix},\ J_{T2} = \begin{bmatrix} -a_1 s_{01} - \frac{a_2}{2} s_{012} & -\frac{a_2}{2} s_{012} \\ a_1 c_{01} + \frac{a_2}{2} c_{012} & \frac{a_2}{2} c_{012} \\ 0 & 0 \end{bmatrix},\ J_{T3} = \begin{bmatrix} -\frac{a_3}{2} s_{03} & 0 \\ \frac{a_3}{2} c_{03} & 0 \\ 0 & 0 \end{bmatrix}$$

Substituting the above values in (C.2) we get

$$p = M v_0 + M \omega_0 \times r_{0g} + J_{Tg} \dot{\theta}; \tag{C.3}$$

where

$M = m_0 + m_1 + m_2 + m_3$

$$r_{0g} = \begin{bmatrix} \frac{m_1}{M} \frac{a_0}{2} c_0 + \frac{m_1}{M} \frac{a_1}{2} c_{01} + \frac{m_2}{M} \frac{a_0}{2} c_0 + \frac{m_2}{M} a_1 c_{01} + \frac{m_2}{M} \frac{a_2}{2} c_{012} + \frac{m_3}{M} \frac{a_0}{2} c_0 + \frac{m_3}{M} \frac{a_3}{2} c_{03} \\ \frac{m_1}{M} \frac{a_0}{2} s_0 + \frac{m_1}{M} \frac{a_1}{2} s_{01} + \frac{m_2}{M} \frac{a_0}{2} s_0 + \frac{m_2}{M} a_1 s_{01} + \frac{m_2}{M} \frac{a_2}{2} s_{012} + \frac{m_3}{M} \frac{a_0}{2} s_0 + \frac{m_3}{M} \frac{a_3}{2} s_{03} \\ 0 \end{bmatrix}$$

$$J_{Tg} = \begin{bmatrix} m_1\frac{a_1}{2}s_{01} - m_2a_1s_{01} - m_2\frac{a_2}{2}s_{012} & -m_2\frac{a_2}{2}s_{012} - m_3\frac{a_3}{2}s_{03} \\ m_1\frac{a_1}{2}c_{01} + m_2a_1c_{01} + m_2\frac{a_2}{2}c_{012} & m_2\frac{a_2}{2}c_{012} + m_3\frac{a_3}{2}c_{03} \\ 0 & 0 \end{bmatrix}$$

Note that the term $J_{Tg}\phi$ represents the linear momentum of the center of mass of the manipulator (without base) as seen from the coordinate frame fixed in the base body.

C.2 ANGULAR MOMENTUM

Angular momentum (l) of the system under study is defined as

$$l = \sum_{i=0}^{n} (I_i\omega_i + r_i \times m_i v_i) \tag{C.4}$$

Alternatively, Angular momentum (l) around the origin of the inertial frame as given in (Dimitrov, 2006) is written as

$$l = Mr_g \times v_0 + I_w\omega_0 + I_\theta\dot{\theta} \tag{C.5}$$

where

$$r_g = \begin{bmatrix} \frac{m_1}{M}\frac{a_0}{2}c_0 + \frac{m_1}{M}\frac{a_1}{2}c_{01} + \frac{m_2}{M}\frac{a_0}{2}c_0 + \frac{m_2}{M}a_1c_{01} + \frac{m_2}{M}\frac{a_2}{2}c_{012} + \frac{m_3}{M}\frac{a_0}{2}c_0 + \frac{m_3}{M}\frac{a_3}{2}c_{03} \\ \frac{m_1}{M}\frac{a_0}{2}s_0 + \frac{m_1}{M}\frac{a_1}{2}s_{01} + \frac{m_2}{M}\frac{a_0}{2}s_0 + \frac{m_2}{M}a_1s_{01} + \frac{m_2}{M}\frac{a_2}{2}s_{012} + \frac{m_3}{M}\frac{a_0}{2}s_0 + \frac{m_3}{M}\frac{a_3}{2}s_{03} \\ 0 \end{bmatrix}$$

$$I_w = I_{1z} + I_{2z} + I_{3z} + m_1r_1r_1^T + m_2r_2r_2^T + m_3r_3r_3^T$$

$$I_\theta = I_{1z}J_{R1} + m_1\hat{r_1}J_{T1} + I_{2z}J_{R2} + m_2\hat{r_2}J_{T2} + I_{3z}J_{R3} + m_3\hat{r_3}J_{T3}$$

In the above expression, I_{0z}, I_{1z}, I_{2z} and I_{3z} is the moment of inertia of link $0, 1, 2$ and 3, respectively about z-axis, $\hat{r_1}, \hat{r_2}$ and $\hat{r_3}$ is skew-symmetric matrix associated with r_1, r_2 and r_3, respectively. The J_{R1}, J_{R2} and J_{R3} is written as

$$J_{R1} = \begin{bmatrix} 0 & 0 \\ 0 & 0 \\ 1 & 0 \end{bmatrix}, J_{R2} = \begin{bmatrix} 0 & 0 \\ 0 & 0 \\ 1 & 1 \end{bmatrix}, J_{R3} = \begin{bmatrix} 0 & 0 \\ 0 & 0 \\ 1 & 0 \end{bmatrix}$$

C.3 MATRIX FORMULATION

Equation (C.2) and (C.5) can be written in a compact matrix from as

$$\begin{bmatrix} p \\ l \end{bmatrix} = \begin{bmatrix} ME & Mr_{og}^T \\ Mr_g & I_w \end{bmatrix} \begin{bmatrix} v_0 \\ \omega_0 \end{bmatrix} + \begin{bmatrix} J_{Tg} \\ I_\theta \end{bmatrix} \dot{\theta} \tag{C.6}$$

In the above equation, E is identity matrix of the compatible dimension. The linear and angular momenta are expressed with respect to origin of inertial frame; the same can also be expressed w.r.t the base centroid as

$$\begin{bmatrix} p_0 \\ l_0 \end{bmatrix} = \begin{bmatrix} p \\ l - r_0 \times p \end{bmatrix} \tag{C.7}$$

Using (C.7), p and l of (C.6) can also alternatively be written as

$$\begin{bmatrix} p \\ l \end{bmatrix} = \begin{bmatrix} ME & Mr_{og}^T \\ Mr_g & I_w \end{bmatrix} \begin{bmatrix} v_0 \\ \omega_0 \end{bmatrix} + \begin{bmatrix} J_{Tg} \\ I_\theta \end{bmatrix} \dot{\theta} + \begin{bmatrix} 0 \\ r_0 \times p \end{bmatrix}$$

$$\begin{bmatrix} p \\ l \end{bmatrix} = I_b t_b + I_{bm1} \dot{\theta}_{m1} + I_{bm2} \dot{\theta}_{m2} + \begin{bmatrix} 0 \\ r_0 \times p \end{bmatrix} \tag{C.8}$$

Here, I_b is the inertia matrix of the floating-base, I_{bm1} and I_{bm2} is the coupling inertia matrices for arm 1 and 2, respectively and r_0 is position vector of center-of-mass.

References

Angeles, J. and Lee, S. K., (1988), "The formulation of dynamical equations of holonomic mechanical systems using a natural orthogonal complement", Journal of applied mechanics, Vol.55, No.1, pp.243–244, 1988

Chapnik, B., Heppler, G. R., and Aplevich, J. D., (1991), "Modeling impact on a one-link flexible robotic arm", IEEE Transactions on Robotics and Automation, Vol.7, No.4, pp.479–488, 1991

Chaudhary, H. and Saha, S. K., (2008), Dynamics and balancing of multibody systems, volume 37, Springer Science & Business Media, 2008

Cyril, X., Jaar, G. J., and Misra, A. K., (1993), "The effect of payload impact on the dynamics of a space robot", In Intelligent Robots and Systems' 93, IROS'93. Proceedings of the 1993 IEEE/RSJ International Conference on, volume 3, pp. 2070–2075, IEEE

Cyril, X., Misra, A. K., Ingham, M., and Jaar, G. J., (2000), "Postcapture dynamics of a spacecraft-manipulator-payload system", Journal of Guidance, Control, and Dynamics, Vol.23, No.1, pp.95–100, 2000

Dimitrov, D., (2006), Dynamics and control of space manipulators during a satellite capturing operation, PhD thesis

Eberhard, P. and Schiehlen, W., (2006), "Computational dynamics of multibody systems: history, formalisms, and applications", Journal of computational and nonlinear dynamics, Vol.1, No.1, pp.3–12, 2006

Featherstone, R. and Orin, D., (2000), "Robot dynamics: equations and algorithms", In Robotics and Automation, 2000. Proceedings. ICRA'00. IEEE International Conference on, volume 1, pp. 826–834, IEEE

Gattupalli, A., Shah, S., Krishna, K. M., and Misra, A., (2013), "Control strategies for reactionless capture of an orbiting object using a satellite mounted robot", In Proceedings of Conference on Advances In Robotics, pp. 1–6, ACM

Gertz, M. W., Kim, J.-O., and Khosla, P. K., (1991), "Exploiting redundancy to reduce impact force", In Intelligent Robots and Systems' 91.'Intelligence for Mechanical Systems, Proceedings IROS'91. IEEE/RSJ International Workshop on, pp. 179–184, IEEE

Goldsmith, W., (1960), "Impact: the Theory and Physical Behaviour of Colliding SolidsEdward Arnold Ltd", London, England„ 1960

Hafez, A. A., Anurag, V., Shah, S., Krishna, K. M., and Jawahar, C., (2014), "Reactionless visual servoing of a dual-arm space robot", In Robotics and Automation (ICRA), 2014 IEEE International Conference on, pp. 4475–4480, IEEE

Hollerbach, J. M., (1980), "A recursive lagrangian formulation of manipulator dynamics", 1980

Lin, Z., Patel, R. V., and Balafoutis, C. A., (1995), "Impact reduction for redundant manipulators using augmented impedance control", Journal of Field Robotics, Vol.12, No.5, pp.301–313, 1995

Liou, J.-C., (2011), "An active debris removal parametric study for LEO environment remediation", Advances in Space Research, Vol.47, No.11, pp.1865–1876, 2011

Liu, S., Wu, L., and Lu, Z., (2007), "Impact dynamics and control of a flexible dual-arm space robot capturing an object", Applied mathematics and computation, Vol.185, No.2, pp.1149–1159, 2007

Nenchev, D. N. and Yoshida, K., (1999), "Impact analysis and post-impact motion control issues of a free-floating space robot subject to a force impulse", IEEE Transactions on Robotics and Automation, Vol.15, No.3, pp.548–557, 1999

Nikravesh, P. E., (1988), Computer-aided analysis of mechanical systems, Prentice-Hall, Inc., 1988

Orin, D. and Walker, M., (1982), "Efficient dynamic computer simulation of robotic mechanisms", ASME Trans. J. dynamics Systems, Measurement and Control, Vol.104„ pp.205–211, 1982

Riley, W. F. and Sturges, L. D., (1996), Engineering mechanics, Wiley, 1996

Saha, S., Shah, S., and Nandihal, P., (2013), "Evolution of the DeNOC-based dynamic modelling for multibody systems", Mechanical Sciences, Vol.4, No.1, pp.1–20, 2013

Saha, S. K., (1996), "A unified approach to space robot kinematics", IEEE transactions on robotics and automation, Vol.12, No.3, pp.401–405, 1996

Saha, S. K., (1997), "A decomposition of the manipulator inertia matrix", IEEE Transactions on Robotics and Automation, Vol.13, No.2, pp.301–304, 1997

Saha, S. K., (1999), "Dynamics of serial multibody systems using the decoupled natural orthogonal complement matrices", Journal of applied mechanics, Vol.66, No.4, pp.986–996, 1999

Schiehlen, W., (1997), "Multibody system dynamics: Roots and perspectives", Multibody system dynamics, Vol.1, No.2, pp.149–188, 1997

Schiehlen, W. et al., (1990), Multibody systems handbook, volume 6, Springer, 1990

Schwertassek, R and Roberson, RE,Dynamics of multibody systems,

Sellmaier, F., Boge, T., Spurmann, J., Gully, S., Rupp, T., and Huber, F., (2010), "On-orbit servicing missions: Challenges and solutions for spacecraft operations", In SpaceOps 2010 Conference Delivering on the Dream Hosted by NASA Marshall Space Flight Center and Organized by AIAA, pp. 2159

Shabana, A. A., (2009), Computational dynamics, John Wiley & Sons, 2009

Shah, S., Saha, S., and Dutt, J., (2012a), "Modular framework for dynamic modeling and analyses of legged robots", Mechanism and Machine Theory, Vol.49„ pp.234–255, 2012

Shah, S. V., Nandihal, P. V., and Saha, S. K., (2012b), "Recursive dynamics simulator (ReDySim): A multibody dynamics solver", Theoretical and Applied Mechanics Letters, Vol.2, No.6, 2012

Stejskal, V. and Valášek, M., (1996), Kinematics and dynamics of machinery, M. Dekker, 1996

Takahashi, R., Ise, H., Konno, A., Uchiyama, M., and Sato, D., (2008), "Hybrid simulation of a dual-arm space robot colliding with a floating object", In Robotics and Automation, 2008. ICRA 2008. IEEE International Conference on, pp. 1201–1206, IEEE

Umetani, Y. and Yoshida, K., (1989), "Resolved motion rate control of space manipulators with generalized Jacobian matrix", IEEE Transactions on robotics and automation, Vol.5, No.3, pp.303–314, 1989

Walker, I. D., (1994), "Impact configurations and measures for kinematically redundant and multiple armed robot systems", IEEE transactions on robotics and automation, Vol.10, No.5, pp.670–683, 1994

Wee, L.-B. and Walker, M. W., (1993), "On the dynamics of contact between space robots and configuration control for impact minimization", IEEE Transactions on Robotics and Automation, Vol.9, No.5, pp.581–591, 1993

Wittenburg, J., (2007), Dynamics of multibody systems, Springer Science & Business Media, 2007

Yoshida, K., Dimitrov, D., and Nakanishi, H., (2006), "On the capture of tumbling satellite by a space robot", In Intelligent Robots and Systems, 2006 IEEE/RSJ International Conference on, pp. 4127–4132, IEEE

Yoshida, K. and Sashida, N., (1993), "Modeling of impact dynamics and impulse minimization for space robots", In Intelligent Robots and Systems' 93, IROS'93. Proceedings of the 1993 IEEE/RSJ International Conference on, volume 3, pp. 2064–2069, IEEE

Youcef-Toumi, K. and Gutz, D. A., (1989), "Impact and force control", In Robotics and Automation, 1989. Proceedings., 1989 IEEE International Conference on, pp. 410–416, IEEE

Zheng, Y.-F. and Hemami, H., (1985), "Mathematical modeling of a robot collision with its environment", Journal of Field Robotics, Vol.2, No.3, pp.289–307, 1985